






# Senolytics improve physical function and increase lifespan in old age

Ming Xu <sup>1,2\*</sup>, Tamar Pirtskhalava<sup>1</sup>, Joshua N. Farr<sup>1</sup>, Bettina M. Weigand<sup>1,3</sup>, Allyson K. Palmer <sup>1</sup>, Megan M. Weivoda<sup>1</sup>, Christina L. Inman<sup>1</sup>, Mikolaj B. Ogrodnik<sup>1,3</sup>, Christine M. Hachfeld<sup>1</sup>, Daniel G. Fraser<sup>1</sup>, Jennifer L. Onken<sup>1</sup>, Kurt O. Johnson<sup>1</sup>, Grace C. Verzosa<sup>1</sup>, Larissa G. P. Langhi<sup>1</sup>, Moritz Weigl<sup>1</sup>, Nino Giorgadze<sup>1</sup>, Nathan K. LeBrasseur<sup>1</sup>, Jordan D. Miller<sup>1</sup>, Diana Jurk<sup>3</sup>, Ravinder J. Singh<sup>4</sup>, David B. Allison <sup>5,6</sup>, Keisuke Ejima <sup>5,6</sup>, Gene B. Hubbard<sup>7</sup>, Yuji Ikeno<sup>7,8</sup>, Hajrunisa Cubro<sup>9</sup>, Vesna D. Garovic<sup>9</sup>, Xiaonan Hou<sup>10</sup>, S. John Weroha<sup>10</sup>, Paul D. Robbins<sup>11</sup>, Laura J. Niedernhofer<sup>11</sup>, Sundeep Khosla <sup>1</sup>, Tamara Tchkonja<sup>1\*</sup> and James L. Kirkland<sup>1\*</sup>

**Physical function declines in old age, portending disability, increased health expenditures, and mortality. Cellular senescence, leading to tissue dysfunction, may contribute to these consequences of aging, but whether senescence can directly drive age-related pathology and be therapeutically targeted is still unclear. Here we demonstrate that transplanting relatively small numbers of senescent cells into young mice is sufficient to cause persistent physical dysfunction, as well as to spread cellular senescence to host tissues. Transplanting even fewer senescent cells had the same effect in older recipients and was accompanied by reduced survival, indicating the potency of senescent cells in shortening health- and lifespan. The senolytic cocktail, dasatinib plus quercetin, which causes selective elimination of senescent cells, decreased the number of naturally occurring senescent cells and their secretion of frailty-related proinflammatory cytokines in explants of human adipose tissue. Moreover, intermittent oral administration of senolytics to both senescent cell-transplanted young mice and naturally aged mice alleviated physical dysfunction and increased post-treatment survival by 36% while reducing mortality hazard to 65%. Our study provides proof-of-concept evidence that senescent cells can cause physical dysfunction and decreased survival even in young mice, while senolytics can enhance remaining health- and lifespan in old mice.**

New approaches to treat age-related diseases (e.g., cardiovascular disease) may yield lifespan extension but potentially at the cost of extending late-life morbidity<sup>1</sup>. A major question in biology is whether interventions can be devised that enhance healthspan in tandem with increasing remaining lifespan so that the period of morbidity near the end of life is not increased<sup>2</sup>. Physical dysfunction and incapacity to respond to stresses<sup>3,4</sup> become increasingly prevalent toward the end of life<sup>5</sup>, with up to 45% of people over the age of 85 being frail<sup>6</sup>. This physical dysfunction is associated with considerable morbidity, including decreased mobility and increased burden of age-related chronic diseases, loss of independence, nursing home and hospital admissions, and mortality<sup>7</sup>. The cellular pathogenesis of age-related physical dysfunction has not been fully elucidated, and there are currently no root cause-directed, mechanism-based interventions for improving physical function in the elderly available for clinical application. Here we report a potential strategy for addressing this need: reducing senescent cell burden.

Cellular senescence is a cell fate involving extensive changes in gene expression and proliferative arrest. Senescence can be induced by such stresses as DNA damage, telomere shortening, oncogenic mutations, metabolic and mitochondrial dysfunction, and inflammation<sup>8–10</sup>. Senescent cell burden increases in multiple tissues with aging<sup>11</sup>, at sites of pathology in multiple chronic diseases, and after radiation or chemotherapy<sup>12</sup>. Senescent cells can secrete a range of proinflammatory cytokines, chemokines, proteases, and other factors; together, these are termed the senescence-associated secretory phenotype (SASP)<sup>13,14</sup>, which contributes to local and systemic dysfunction with aging and in a number of diseases<sup>15–21</sup>. A month or more of continuous treatment with Janus kinase 1 (JAK1) and JAK2 inhibitors or rapamycin can enhance physical function in older mice<sup>14,22</sup>. However, JAK1 and JAK2 inhibitors and rapamycin have an extensive range of effects on cellular function. Among these is reduced production of some SASP components. We hypothesized, on the basis of these points, that senescent cells might potentially contribute to age-related physical

<sup>1</sup>Robert and Arlene Kogod Center on Aging, Mayo Clinic, Rochester, MN, USA. <sup>2</sup>University of Connecticut Center on Aging, University of Connecticut Health, Farmington, CT, USA. <sup>3</sup>Newcastle University Institute for Ageing and Institute for Cell and Molecular Biosciences, Newcastle University, Newcastle upon Tyne, UK. <sup>4</sup>Department of Laboratory Medicine and Pathology, Mayo Clinic, Rochester, MN, USA. <sup>5</sup>Department of Epidemiology & Biostatistics, School of Public Health, Indiana University–Bloomington, Bloomington, IN, USA. <sup>6</sup>Nathan Shock Center on Comparative Energetics and Aging, University of Alabama at Birmingham, Birmingham, AL, USA. <sup>7</sup>Barshop Institute for Longevity and Aging Studies and Department of Pathology, University of Texas Health Science Center at San Antonio, San Antonio, TX, USA. <sup>8</sup>Geriatric Research Education and Clinical Center, South Texas Veterans Healthcare System, San Antonio, TX, USA. <sup>9</sup>Department of Internal Medicine, Division of Nephrology and Hypertension, Mayo Clinic, Rochester, MN, USA. <sup>10</sup>Department of Oncology, Mayo Clinic, Rochester, MN, USA. <sup>11</sup>Department of Molecular Medicine, Center on Aging, Scripps Research Institute, Jupiter, FL, USA.

\*e-mail: [mixu@uchc.edu](mailto:mixu@uchc.edu); [tchkonja.tamar@mayo.edu](mailto:tchkonja.tamar@mayo.edu); [kirkland.james@mayo.edu](mailto:kirkland.james@mayo.edu)

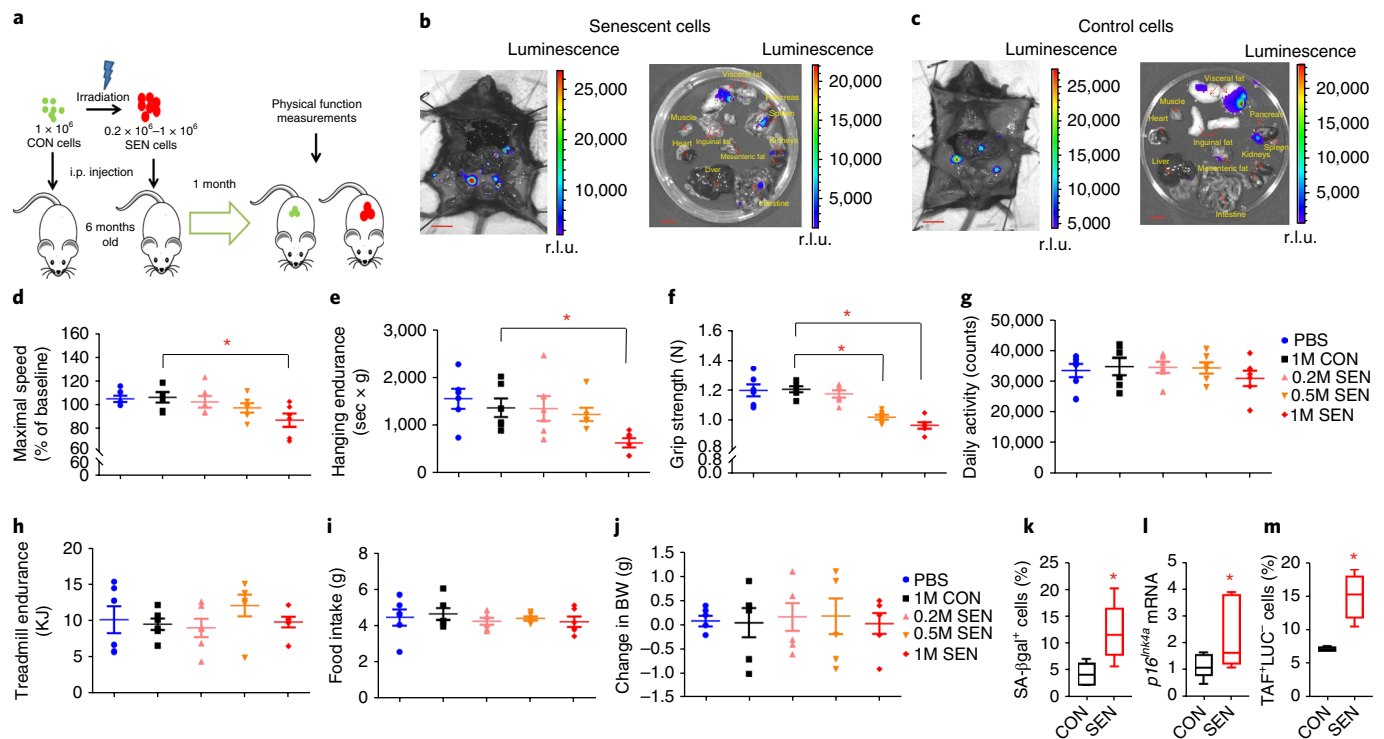


**Fig. 1 | Transplanting small numbers of senescent cells induces physical dysfunction in younger mice.** **a**, Experimental design for transplantation and physical function measurements. i.p., intraperitoneal injection. CON, nonsenescent control cells. SEN, senescent cells. **b,c**, Representative images of LUC activity of various organs from LUC<sup>-</sup> male mice ( $n=3$ ) 5 d post-transplantation with senescent (induced by radiation) (**b**) or control (**c**) preadipocytes from LUC<sup>+</sup> transgenic mice. Scale bars, 10 mm. r.l.u., relative luciferase units. **d–j**, Maximal walking speed (relative to baseline) (**d**), hanging endurance (**e**), grip strength (**f**), daily activity (**g**), treadmill endurance (**h**), food intake (**i**), and change in body weight (BW) (**j**) of 6-month-old male C57BL/6 mice at 1 month after being injected with PBS,  $1 \times 10^6$  nonsenescent control (1M CON),  $0.2 \times 10^6$  senescent (0.2M SEN),  $0.5 \times 10^6$  senescent (0.5M SEN), or  $1 \times 10^6$  senescent (1M SEN) preadipocytes ( $n=6$  mice for all groups). Results are means  $\pm$  s.e.m. **k–m**, Quantification of SA- $\beta$ gal<sup>+</sup> cells among total cells ( $n=6$  mice) (**k**), relative *p16<sup>INK4a</sup>* mRNA levels ( $n=7$  mice) (**l**), and cells from recipient mice that were TAF<sup>+</sup> ( $>2$  TAFs/nucleus) and LUC<sup>-</sup> ( $n=4$  mice) (**m**) in 6-month-old male WT (LUC<sup>-</sup>) C57BL/6 mice 2 months after being transplanted with  $1 \times 10^6$  senescent or control LUC<sup>+</sup> preadipocytes from transgenic mouse donors. Results are shown as box-and-whisker plots, where a box extends from the 25th to 75th percentile with the median shown as a line in the middle, and whiskers indicate the smallest and largest values. \* $P < 0.05$ ; ANOVA with Tukey's post hoc comparison (**d–j**) and two-tailed, unpaired Student's *t*-test (**k–m**).

dysfunction and, if so, that targeting them therapeutically could improve life- and healthspan.

## Results

**Transplanting small numbers of senescent cells is sufficient to induce physical dysfunction in young mice.** To test whether senescent cells can directly cause physical dysfunction, we first transplanted senescent or control (nonsenescent) preadipocytes (also termed adipocyte progenitors or adipose-derived stem cells<sup>23</sup>) isolated from luciferase-expressing transgenic (LUC<sup>+</sup>) mice intraperitoneally into syngeneic, young (6-month-old) wild-type (WT) mice (Fig. 1a). We induced cellular senescence using 10 Gy radiation, which resulted in more than 85% of cells becoming senescent (Supplementary Fig. 1a,b). We transplanted preadipocytes because: (i) the SASP of radiation-induced senescent mouse preadipocytes (Supplementary Fig. 1c,d) resembles that of endogenous senescent cells with aging (Supplementary Fig. 1e)<sup>20,24</sup> and in idiopathic pulmonary fibrosis<sup>25</sup>; (ii) preadipocytes are less immunogenic or subject to rejection than other cell types<sup>26</sup>; and (iii) these cells are arguably the most abundant type of progenitors in humans<sup>27</sup> that are subject to cellular senescence. We also used doxorubicin to induce senescence to ascertain whether the physiological impact of transplanted senescent cells is limited to the context of radiation-induced senescence: senescent cells induced by doxorubicin developed a SASP similar to that of radiation-induced senescent cells (Supplementary Fig. 1f).

Five days after intraperitoneal transplantation of senescent or control preadipocytes, the cells were mainly located in visceral fat (Fig. 1b,c and Supplementary Fig. 2a,b). Both the senescent and control transplanted cells remained detectable through in vivo bioluminescence imaging (BLI) for up to 40 d following transplant (Supplementary Fig. 2c). Of note, we observed that senescent cells had higher luciferase activity than control cells, even though they were from the same LUC<sup>+</sup> transgenic mice (Supplementary Fig. 2d).

To determine whether the transplanted senescent cells induced physical dysfunction in these mice, as determined by criteria used in clinical practice<sup>4</sup>, we measured maximal walking speed (via RotaRod), muscle strength (via grip strength), physical endurance (via hanging test and treadmill), daily activity, food intake, and body weight. Previously healthy young adult mice transplanted with  $10^6$  senescent cells had significantly lower maximal walking speed, hanging endurance, and grip strength by 1 month after transplantation compared to mice transplanted with control cells (Fig. 1d–f and Supplementary Fig. 3a). Transplanting the same number of control cells had no effect as compared to injecting PBS. Daily activity, treadmill performance, food intake, and body weight were not statistically different among groups (Fig. 1g–j). Transplanting  $0.5 \times 10^6$  senescent cells was sufficient to cause decreased grip strength (Fig. 1f) and maximal walking speed (Supplementary Fig. 3b), whereas transplanting  $0.2 \times 10^6$  senescent cells had no detectable effects. Thus, senescent cells can impair physical function

in a dose-dependent manner. We estimate that 6-month-old mice have  $7 \times 10^9$ – $8 \times 10^9$  cells of all types and that the total cell number in intraperitoneal adipose tissue, where the transplanted cells were mainly located (Supplementary Fig. 2b), is  $\sim 3.5 \times 10^8$ – $6 \times 10^8$  cells (Methods). Thus in young mice, if only 1 cell in the 7,000–15,000 (0.01–0.03%) throughout the body or 1 cell in 350 (0.28%) locally is a transplanted senescent cell, age-related impairment in physical function ensues.

Reduced walking speed began as early as 2 weeks following a single implantation of senescent cells (Supplementary Fig. 3c) and persisted for up to 6 months (Supplementary Fig. 3d), yet the transplanted cells survived in vivo for only approximately 40 d, consistent with the possibility that senescent cells might induce senescence in normal host cells<sup>28,29</sup>. We therefore tested whether senescent cells can indeed cause other cells to become senescent in vivo by transplanting constitutively LUC<sup>+</sup> senescent cells and determining whether senescence occurs in the LUC<sup>-</sup> recipients' tissue. Most of the transplanted LUC<sup>+</sup> senescent cells resided in visceral fat (Supplementary Fig. 2b). Two months after transplantation, we found more senescence-associated  $\beta$ -galactosidase (SA- $\beta$ gal)<sup>+</sup> cells and higher cyclin-dependent kinase inhibitor 2A (*Cdkn2a*; also known as *p16<sup>INK4a</sup>*) expression in visceral adipose tissue from senescent cell- than control cell-transplanted mice (Fig. 1k,l) beyond the time the transplanted senescent cells were present as reflected by luciferase signal (Supplementary Fig. 2c). Telomere-associated foci (TAFs) are sites of DNA damage within telomeres<sup>30</sup>. TAFs appear to be a more specific marker of senescence than some others, such as SA- $\beta$ gal. Significantly more TAF<sup>+</sup> cells were found in visceral adipose tissue of mice that had been injected with senescent than control cells (Fig. 1m). These TAF<sup>+</sup> cells were LUC<sup>-</sup>, indicating that they were the recipients' own cells and not transplanted cells. F4/80<sup>+</sup> macrophage accumulation was not induced in adipose tissue by the intraperitoneal senescent cell transplantation (Supplementary Fig. 3e,f). Consistent with spread of senescence not only locally but also to distant tissues, expression of the markers and mediators of senescence *p16<sup>INK4a</sup>*, tumor necrosis factor alpha (*Tnfa*), and interleukin 6 (*Il6*) was higher in the quadriceps muscles, a tissue where transplanted cells were not detected (Supplementary Fig. 2b), of senescent- than control-transplanted mice (Supplementary Fig. 4a). Similarly to adipose tissue, F4/80<sup>+</sup> macrophage accumulation was not induced in muscle by senescent cell transplantation (Supplementary Fig. 4b). Thus, senescence spreading may explain how a small number of transplanted SEN cells caused such profound, long-lasting, and deleterious systemic effects.

To further test whether SASP-related factors can contribute to induction of cellular senescence in vivo, we examined IL-10 knockout mice, which have a genetically induced premature proinflammatory phenotype that resembles the SASP and which also prematurely develop physical dysfunction reminiscent of human frailty<sup>31</sup>. We found that these mice do indeed have more senescent cells than WT controls, supporting the possibility that the SASP can induce senescence spreading in vivo (Supplementary Fig. 5a–c).

**Aging and high-fat diet exacerbate effects of senescent cell transplantation.** Because aging is associated with senescent cell accumulation<sup>14</sup>, we tested whether increased recipient age potentiates the effects of transplanting senescent cells. We transplanted  $0.5 \times 10^6$  senescent or control preadipocytes into older (17-month-old) mice, so that 0.007% of all cells in the recipients were transplanted senescent or control cells, and 1 month later, we measured various parameters of physical function (Fig. 2a). We found that mice transplanted with senescent cells had lower maximal walking speed, hanging endurance, and grip strength than control mice (Fig. 2b–d). These findings were consistent across several independent cohorts of male (Supplementary Fig. 6a–f) and female mice (Supplementary Fig. 6g–l). Body weight, treadmill performance, daily activity, and

food intake were not statistically different after transplanting senescent cells into the older mice (Fig. 2e–h). Transplanting  $0.5 \times 10^6$  senescent cells led to greater impairment in walking speed and hanging endurance in 17-month-old mice than 6-month-old mice (Fig. 2i), whereas other parameters showed no statistically significant difference. Notably, in the 17-month-old mice transplanted with senescent cells, survival for the following year was significantly lower than that of age-matched control mice, with a 5.2-fold higher risk of death (mortality hazard ratio,  $P=0.006$ ) (Fig. 2j). Tumor burden, disease burden at death, and causes of death were not significantly altered by transplantation with senescent cells compared to control cells (Fig. 2k,l), suggesting that a small number of senescent cells may shorten survival through a general process, such as hastening the progression of aging, rather than by inducing any one individual disease or a few individual diseases. Thus, augmenting senescent cell burden induces physical dysfunction, more so in middle-aged than younger individuals, and increases mortality.

To determine whether augmenting senescent cell burden reduces resilience in the face of high fat intake, which is a metabolic stress known to promote senescent cell accumulation<sup>32</sup>, senescent or control preadipocytes were transplanted into 8-month-old nonobese mice, which were then fed a high-fat diet (HFD) for 1 month, followed by measurements of physical function (Fig. 3a). The HFD-fed mice transplanted with  $0.4 \times 10^6$  senescent cells had lower maximal walking speed, hanging endurance, grip strength, daily activity, and food intake compared to HFD-fed mice transplanted with  $0.4 \times 10^6$  control cells (Fig. 3b–f). Body weight and treadmill performance were not statistically different (Fig. 3g,h). Senescent cell-transplanted mice on a HFD had more impairment in walking speed and hanging endurance than age-matched transplanted mice on a normal chow diet (NCD), whereas other parameters were not statistically significantly changed (Fig. 3i). Collectively, these data indicate that transplanting small numbers of senescent cells causes greater systemic dysfunction in older individuals or in the context of metabolic stress.

To test whether the physical dysfunction in mice transplanted with senescent cells was due to transplant rejection, we transplanted mice with autologous ear fibroblasts in which senescence had been induced by 10 Gy radiation<sup>16</sup> versus sham-radiated control cells. Senescent fibroblasts<sup>16</sup> have a similar SASP to senescent preadipocytes (Supplementary Fig. 1c). We transplanted  $10^6$  senescent or control cells back into the same mice from which the ear fibroblasts had been isolated, and these mice were put on a HFD for 1 month (Fig. 3j). Transplanting autologous senescent ear fibroblasts intraperitoneally, compared to control cells, led to impaired maximal walking speed, hanging endurance, and grip strength (Fig. 3k–q), as had occurred after transplanting nonautologous senescent preadipocytes. Moreover, we transplanted radiation-induced senescent primary human preadipocytes (characterized in ref.<sup>14</sup>) versus sham-radiated control cells into severe combined immunodeficiency-beige (SCID-beige) mice with impaired T cell, B cell, and natural killer cell function<sup>33</sup>. Similarly to the effect of mouse senescent cells on immunocompetent mice, we found that physical function was impaired in the immune-deficient mice transplanted with the human senescent cells compared to those treated with control cells or with PBS (Supplementary Fig. 7). Combined with our finding that senescent and control cells persisted for the same amount of time after transplantation (Supplementary Fig. 2c), these data support the possibility that physical dysfunction did not arise principally as a consequence of transplant immune rejection or in response to a particular type of senescent cell.

**Dasatinib plus quercetin reduces senescent cell burden and decreases proinflammatory cytokine secretion in human adipose tissue.** In light of our finding that senescent cells cause physical dysfunction and shorten survival, senolytic agents, which can selectively

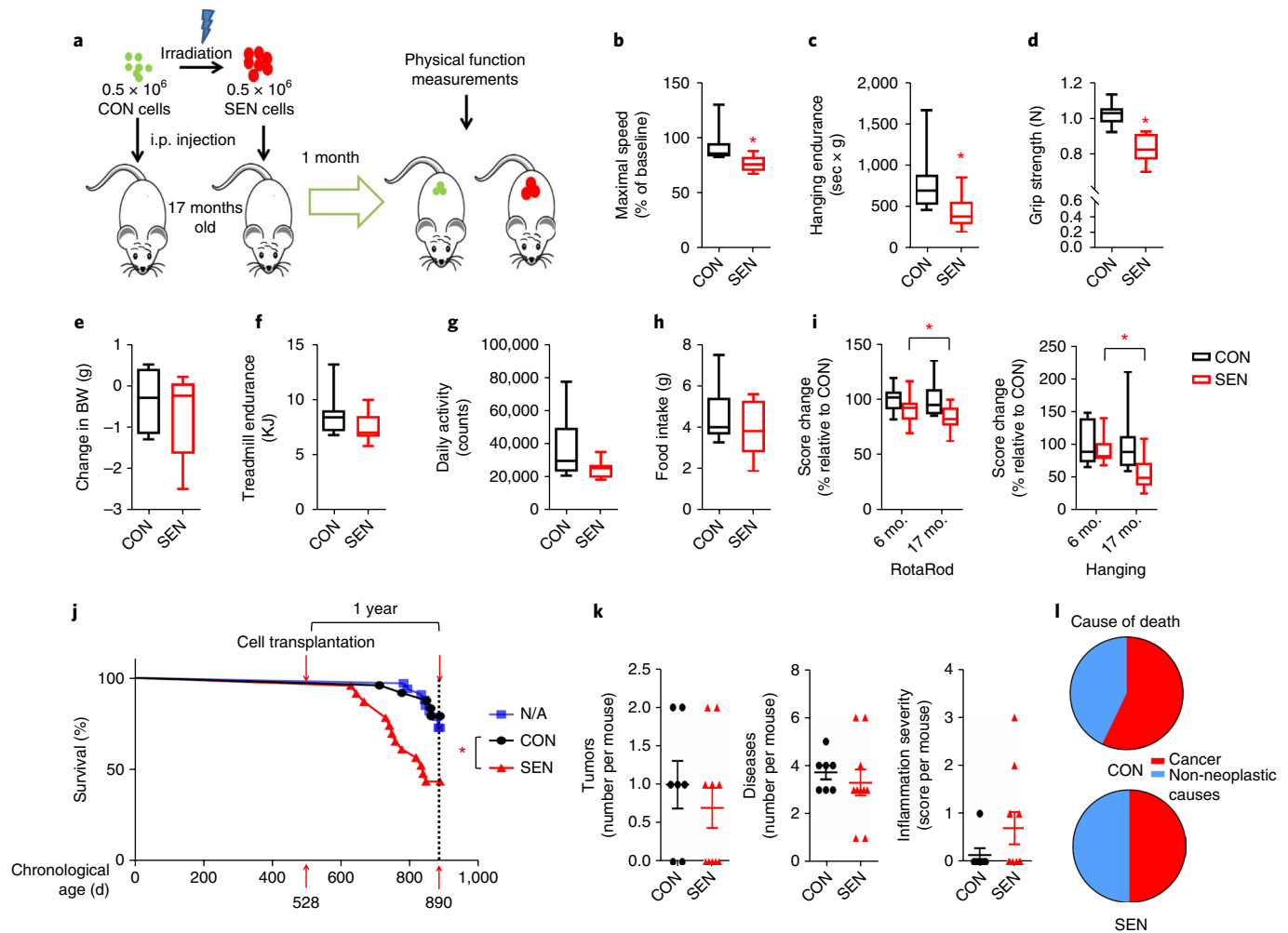


**Fig. 2 | Aging exacerbates the effects of senescent cell transplantation.** **a**, Experimental design for transplantation and physical function measurements. **b-h**, Quantification of maximal walking speed (relative to baseline) (**b**), hanging endurance (**c**), grip strength (**d**), body weight change from baseline (**e**), treadmill endurance (**f**), daily activity (**g**), and food intake (**h**) of 17-month-old male C57BL/6 mice at 1 month after being injected with  $0.5 \times 10^6$  senescent or control preadipocytes ( $n=8$  mice for both groups). **i**, Percent changes in RotaRod (left; in 6-month-old mice,  $n=21$  for both SEN and CON; in 17-month-old mice,  $n=22$  for SEN and  $n=20$  for CON) and hanging test (right; in 6-month-old mice,  $n=6$  for both SEN and CON; in 17-month-old mice,  $n=8$  for both SEN and CON) scores for mice transplanted with  $0.5 \times 10^6$  senescent cells relative to the average of mice transplanted with  $0.5 \times 10^6$  control cells at both ages. Results are shown as box-and-whisker plots, where a box extends from the 25th to 75th percentile with the median shown as a line in the middle, and whiskers indicate the smallest and largest values. **j**, One-year-survival curves of 17-month-old nontransplanted mice ( $n=33$  mice, N/A) and mice transplanted with  $0.5 \times 10^6$  senescent ( $n=23$  SEN mice) or control ( $n=24$  CON mice) preadipocytes. **k**, Quantification of tumor burden (left), disease burden (middle), and inflammation at death (right) (shown as means  $\pm$  s.e.m.) after transplanting senescent or control cells ( $n=10$  SEN mice,  $n=7$  CON mice). **l**, Causes of death in transplanted mice ( $n=10$  SEN mice,  $n=7$  CON mice). \* $P < 0.05$ ; two-tailed unpaired Student's *t*-test (**b-i**, **k**), Cox proportional hazard regression model (**j**) and chi-square and Fisher's exact tests (**l**).

eliminate senescent cells, might be an approach for enhancing healthspan in old individuals. Senolytic drugs have been reported to alleviate a variety of age-related disorders (reviewed in ref.<sup>34</sup>). These agents were originally selected on the basis of their ability to transiently disable the senescence-associated antiapoptotic pathways (SCAPs) that protect senescent cells from their proapoptotic micro-environment<sup>35</sup>. However, the efficacy of senolytics in human tissues remains unclear. To begin the process of gauging the translational potential of this approach, we determined whether the combination of dasatinib plus quercetin (D + Q), the first senolytics reported<sup>35</sup>, is effective in a human tissue. We did so using freshly isolated human omental adipose tissue obtained from obese individuals (body mass index (BMI),  $45.5 \pm 9.1$  kg/m<sup>2</sup>; age,  $45.7 \pm 8.3$  years), as obesity is associated with senescent cell accumulation<sup>27,32</sup>. The surgically excised explants, which indeed contained naturally occurring senescent cells (Supplementary Fig. 8a), were immediately treated

with D + Q (1  $\mu$ M + 20  $\mu$ M) or vehicle for 48 h (Fig. 4a). The explants treated with D + Q had significantly less TAF<sup>+</sup>, p16<sup>INK4A-hi</sup>, and SA- $\beta$ gal<sup>+</sup> cells (Fig. 4b-d) and also more cells undergoing apoptosis (Fig. 4e and Supplementary Fig. 8b) compared to vehicle-treated explants from the same subjects. Forty-eight hours of treatment with vehicle did not affect total and senescent cell numbers in these adipose tissue explants (Supplementary Fig. 8c). Notably, expression levels of the three senescence markers TAF, p16<sup>INK4A</sup>, and SA- $\beta$ gal correlated with each other (Supplementary Fig. 8d).

We next examined whether D + Q had acute effects on macrophages in these explants. We costained for p16<sup>INK4A</sup> and F4/80 (EMR1 in humans). Only the p16<sup>INK4A+</sup>;F4/80(EMR1)<sup>-</sup> cell population was lower in the explants treated with D + Q than in those treated with vehicle, whereas the numbers of p16<sup>INK4A+</sup>;F4/80(EMR1)<sup>+</sup> or p16<sup>INK4A-</sup>;F4/80(EMR1)<sup>+</sup> cells were not significantly affected (Supplementary Fig. 9a). In addition, expression of CD68, another

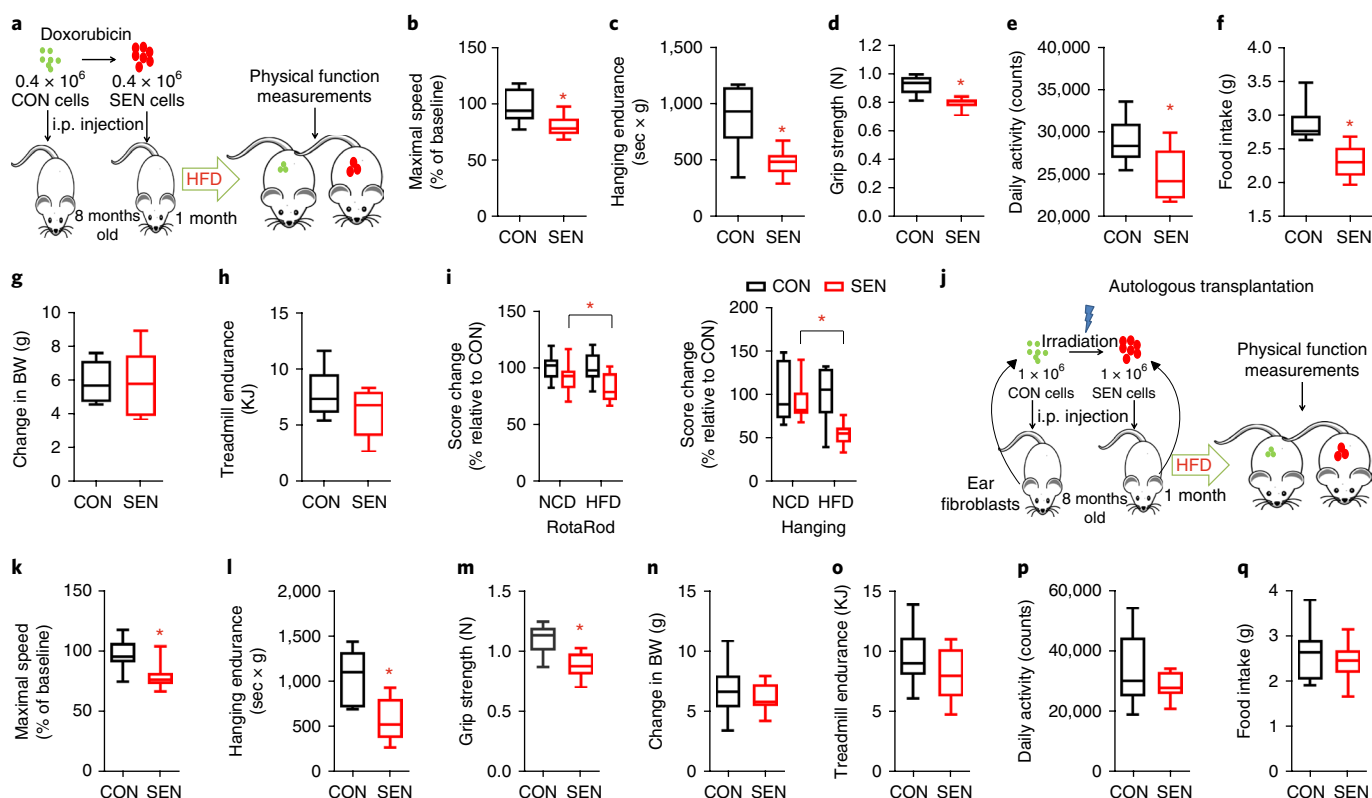


**Fig. 3 | Senescent cells reduce resilience to metabolic stress in mice.** **a**, Experimental design for transplantation and physical function measurements. **b–h**, Quantification of maximal walking speed (relative to baseline) (**b**), hanging endurance (**c**), grip strength (**d**), daily activity (**e**), food intake (**f**), body weight change from baseline (**g**), and treadmill endurance (**h**) of 8-month-old male C57BL/6 mice fed a HFD for 1 month that were injected with  $0.4 \times 10^6$  senescent or control preadipocytes ( $n=6$  mice for both groups). **i**, Percent changes in RotaRod (left; on NCD,  $n=21$  mice for both SEN and CON; on HFD,  $n=12$  mice for both SEN and CON) and hanging test (right; on NCD,  $n=6$  for both SEN and CON; on HFD,  $n=6$  for both SEN and CON) scores in HFD- and NCD-fed mice transplanted with  $0.4 \times 10^6$ – $0.5 \times 10^6$  senescent cells relative to the average of mice transplanted with  $0.4 \times 10^6$ – $0.5 \times 10^6$  control cells. **j**, Experimental design for transplantation and physical function measurements. **k–q**, Quantification of maximal walking speed (relative to baseline) (**k**), hanging endurance (**l**), grip strength (**m**), body weight change from baseline (**n**), treadmill endurance (**o**), daily activity (**p**), and food intake (**q**) of 8-month-old male C57BL/6 mice injected with  $1 \times 10^6$  senescent or control autologous ear fibroblasts ( $n=10$  for both groups) at 1 month on a HFD. All results are shown as box-and-whisker plots, where a box extends from the 25th to 75th percentile with the median shown as a line in the middle, and whiskers indicate the smallest and largest values. \* $P < 0.05$ ; two-tailed unpaired Student's *t*-tests (**b–i, k–q**).

macrophage marker was not altered acutely by D+Q in the adipose tissue explants (Supplementary Fig. 9b). These data suggest that D+Q treatment has little direct effect on macrophages, including  $p16^{\text{INK4A}}$  macrophages.

Senescent preadipocytes produce a variety of proinflammatory cytokines<sup>14</sup> and can also induce cytokine production by adipose tissue in vitro (Supplementary Fig. 10), potentially leading to amplification of adipose tissue inflammation. To test whether D+Q decreases cytokine secretion by adipose tissue from obese individuals, we treated explants with D+Q or vehicle for 48 h and then washed the explants. Conditioned medium (CM) was collected in the absence of drugs over the next 24 h. We measured secreted protein levels in CM after D+Q treatment and found less secretion of the key SASP components<sup>14</sup> IL-6, IL-8, monocyte chemoattractant protein 1 (MCP-1), plasminogen activator inhibitor 1 (PAI-1), and granulocyte macrophage colony-stimulating factor (GM-CSF) in CM from the D+Q group than from the vehicle group, whereas two non-SASP-related factors, IL-10 and interferon (IFN)- $\gamma$  (ref.<sup>14</sup>), were not statistically significantly altered (Fig. 4f and Supplementary Fig. 11a). Furthermore, secretion of two adipokines, adiponectin and adipisin (markers of adipose tissue function<sup>36</sup>), were not lower in the D+Q group, excluding a nonspecific effect of D+Q on protein secretion or overall cell viability (Fig. 4f). D+Q increased expression of peroxisome proliferator-activated receptor  $\gamma$  (PPAR $\gamma$ ) and

CEBP $\alpha$ , two key transcription factors that are required for adipose tissue function through regulating adipogenesis and adipose tissue insulin responsiveness<sup>15,37</sup> (Fig. 4g). This parallels the induction of these key adipogenic factors that we previously reported after targeting cellular senescence either by clearing senescent cells genetically from transgenic INK-ATTAC mice or inhibiting the SASP<sup>15</sup>. D+Q reduced cytokine production more extensively in the human adipose tissue explants than either D or Q alone (Supplementary Fig. 11b), consistent with the finding that D+Q target a broader range of senescent cells than D or Q alone<sup>35</sup>. Of note, increases in IL-6 (ref.<sup>38,39</sup>), MCP-1 (ref.<sup>40,41</sup>), and  $p16^{\text{INK4A}}$  (ref.<sup>42,43</sup>) are associated with frailty in humans. Thus, it appears that D+Q can kill naturally occurring human senescent cells and can attenuate secretion of inflammatory cytokines associated with human age-related frailty.

**Eliminating senescent cells both prevents and alleviates physical dysfunction induced by senescent cell transplantation.** We tested whether D+Q kills transplanted senescent cells in vivo by injecting LUC<sup>+</sup> senescent or control preadipocytes intraperitoneally into non-luciferase-expressing WT mice. The mice were treated immediately after transplantation with D+Q or vehicle for 3 d (Fig. 5a). Luminescence was significantly lower in senescent cell-transplanted mice treated with D+Q than in vehicle-treated mice, and no difference was observed following treatment of mice

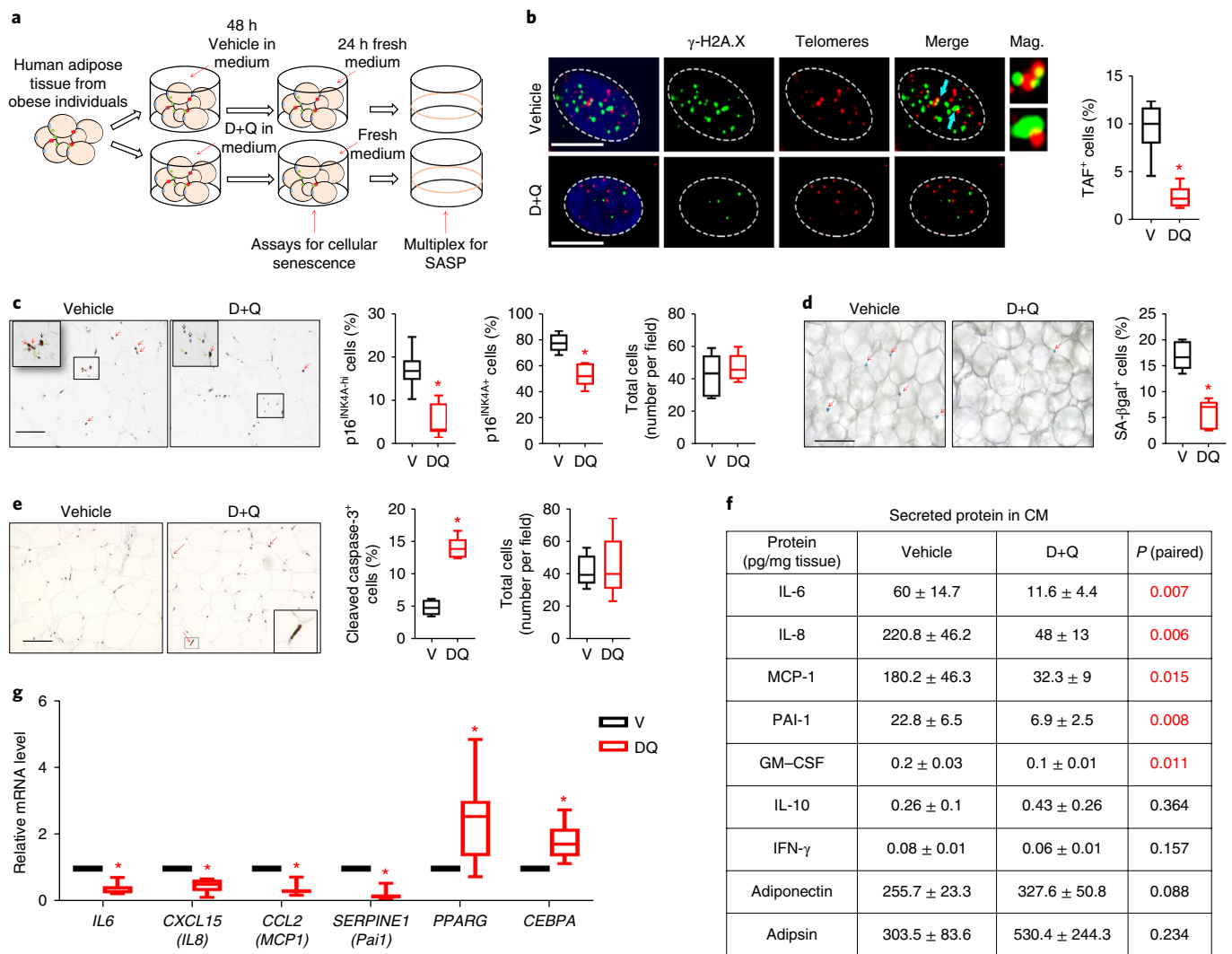


**Fig. 4 | D + Q reduces senescent cell abundance and decreases proinflammatory cytokine secretion in human adipose tissue.** **a**, Experimental design for the human adipose tissue explant experiment. **b**, Right, Micrographs of adipose tissue explants in D + Q (DQ)- and vehicle-treated samples. Gamma-H2A.X (the phosphorylated form of H2A histone family member X) foci, which indicate DNA damage, are stained green. Telomeres are stained red. Blue arrows indicate TAFs, which are shown in the 10× high-magnification images (Mag.). The white dashed line outlines the cell nucleus. Scale bars, 5 μm. Right, Quantification of TAF<sup>+</sup> cells among total cells (explant tissue from *n* = 5 subjects). **c**, Left, Micrographs of adipose tissue explants in D + Q- and vehicle-treated samples. Red arrows, p16<sup>INK4A</sup>-hi cells; green arrows, p16<sup>INK4A</sup>+ cells (expressing any detectable level of p16<sup>INK4A</sup>); black arrows, p16<sup>INK4A</sup>- cells. Right, Quantification of p16<sup>INK4A</sup>+ and p16<sup>INK4A</sup>-hi cells among total cells and cell number per field (explant tissue from *n* = 6 subjects). Scale bar, 100 μm. **d**, Left, Micrographs of adipose tissue explants in D + Q- and vehicle-treated samples. Red arrows, SA-βgal<sup>+</sup> cells. Scale bar, 100 μm. Right, Quantification of SA-βgal<sup>+</sup> cells among total cells (explant tissue from *n* = 6 subjects). **e**, Left, Micrographs of adipose tissue explants in D + Q- and vehicle-treated samples. Red arrows, cleaved caspase-3<sup>+</sup> cells. Scale bar, 100 μm. Right, Quantification of cleaved caspase-3<sup>+</sup> cells among total cells and cell number per field (explant tissue from *n* = 5 subjects). **f**, Secreted cytokine and adipokine levels in CM (explant tissue from *n* = 8 subjects). Results are means ± s.e.m. Significant comparisons are shown in red. **g**, The relative mRNA abundance of genes encoding key SASP components and markers for adipose tissue function (explant tissue from *n* = 7 subjects). All results are shown as box-and-whisker plots, where a box extends from the 25th to 75th percentile with the median shown as a line in the middle, and whiskers indicate the smallest and largest values. \**P* < 0.05; two-tailed Student's *t*-tests (**b-g**).

transplanted with LUC<sup>+</sup> control cells (Fig. 5b,c), confirming D + Q are senolytic in vivo. These findings further support the conclusion that D + Q can selectively kill senescent cells.

We ascertained whether clearing transplanted senescent cells using D + Q prevents development of physical dysfunction. Treating young mice with D + Q at the time of senescent cell transplantation for 3 d attenuated the deteriorations in walking speed, hanging endurance, and grip strength that occurred 1 month later in vehicle-treated senescent cell-transplanted mice, consistent with the possibility that D + Q treatment is sufficient to prevent the physical dysfunction caused by senescent cells (Fig. 5d-f). D + Q

also alleviated the physical dysfunction that occurred in mice at 5 weeks following senescent cell transplantation (Fig. 5g). In the senescent cell-transplanted mice, a single 5-d course of D + Q treatment improved physical function compared to vehicle (Fig. 5h-j). This improvement was evident at 2 weeks after D + Q treatment and lasted for several months (Supplementary Fig. 12a). At these two time points of D + Q administration (immediately versus 5 weeks after transplantation), the beneficial effects of D + Q were comparable. Therefore, we speculate that the time of administration of senolytics may be flexible, potentially increasing their clinical utility. Because D + Q have elimination half-lives of < 12 h<sup>44,45</sup>, this

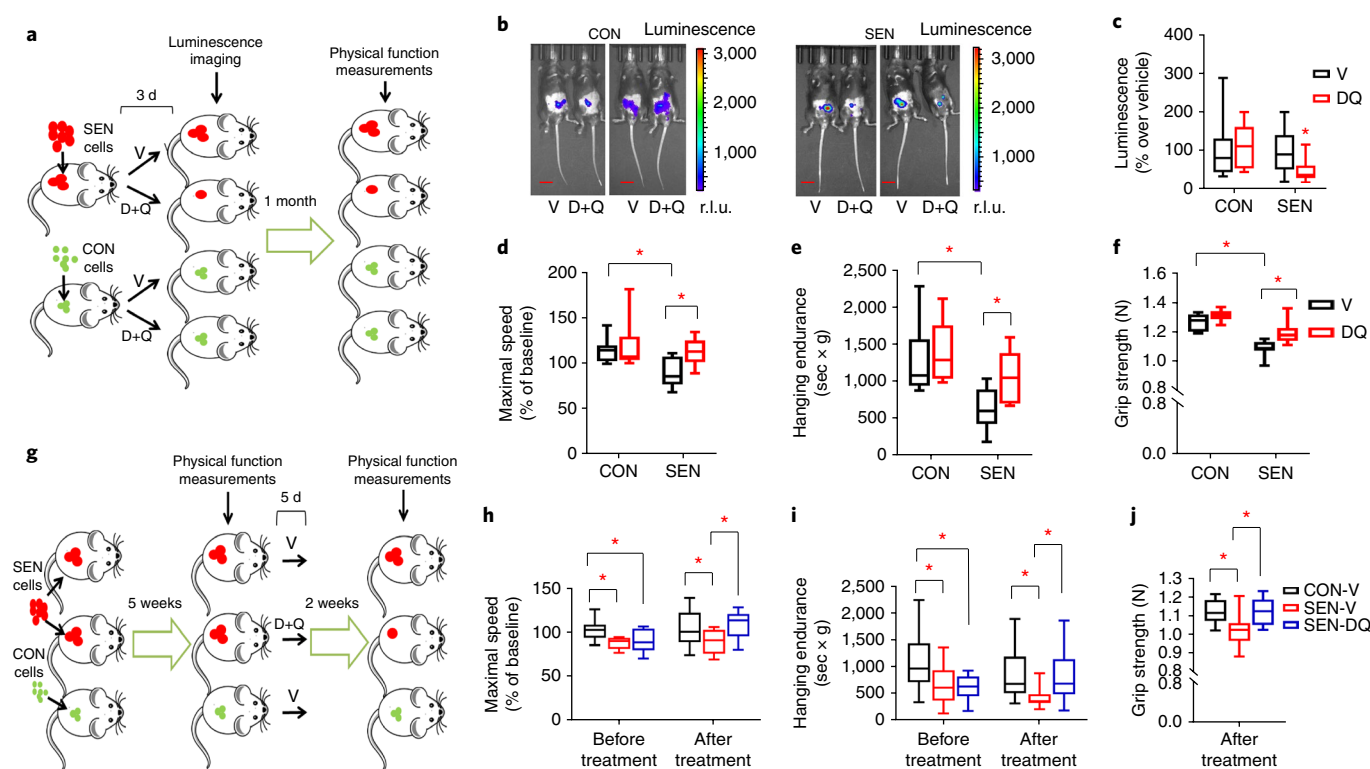


**Fig. 5 | Eliminating senescent cells both prevents and alleviates physical dysfunction.** **a**, Experimental design for transplantation and physical function measurements. **b**, Representative images showing LUC activity in mice at 2 d after the last treatment. Scale bars, 15 mm. **c**, Luminescence of transplanted cells as a percentage relative to the average of mice treated with vehicle ( $n=16$  for SEN-DQ vehicle SEN-V;  $n=13$  for CON-DQ versus CON-V). **d–f**, Quantification of maximal walking speed (relative to baseline) (**d**), hanging endurance (**e**), and grip strength (**f**) of 5-month-old male C57BL/6 mice 1 month after the last drug treatment ( $n=7$  for SEN-V, CON-V, and SEN-DQ;  $n=6$  for CON-DQ). **g**, Experimental design for transplantation and physical function measurements. **h–j**, Quantification of maximal walking speed (relative to baseline) (**h**), hanging endurance (**i**), and grip strength (**j**) of 5-month-old male C57BL/6 mice 2 weeks after the last drug treatment ( $n=10$  for SEN-DQ and SEN-V;  $n=14$  for CON-V). All results are shown as box-and-whisker plots, where a box extends from the 25th to 75th percentile with the median shown as a line in the middle, and whiskers indicate smallest and largest values. \* $P < 0.05$ ; two-tailed Student's  $t$ -tests (**b–f, h–j**).

sustained improvement in physical function following a single course of D + Q treatment does not involve mechanisms that require continuous presence of the drugs, such as occupancy of a receptor or sustained effects on an enzyme. These findings suggest that the senolytic activity of D + Q is sufficient to attenuate senescent cell-induced physical dysfunction.

**Clearance of senescent cells alleviates physical dysfunction and increases late-life survival without extending morbidity in aged mice.** D + Q have been shown to decrease senescent cells in a variety of tissues in different situations, including aging<sup>25,35,46–48</sup>. To test the role of senescent cells in physical dysfunction in aged mice, we treated 20-month-old nontransplanted, WT mice with D + Q or vehicle intermittently for 4 months (Fig. 6a). D + Q alleviated physical dysfunction—maximal walking speed, hanging endurance, grip strength, treadmill endurance, and daily activity were higher in mice treated with D + Q than in those treated with vehicle (Fig. 6b–g). Food intake also tended to be higher in D + Q-treated mice ( $P=0.074$ ; Fig. 6h). Moreover, the expression of several key SASP components was lower in the visceral adipose tissue from aged mice treated with D + Q than in vehicle-treated mice (Fig. 6i), concordant with lower secretion of SASP factors by human adipose tissue treated with D + Q (Fig. 4g).

To further test the possibility that there could be a causal role for senescent cells in inducing physical dysfunction, we used the transgenic *INK-ATTAC* mouse model, in which endogenous  $p16^{\text{INK4A}}$  cells, many of which are senescent, can be genetically cleared by

activating the caspase-8 moiety of ATTAC, which is expressed only in  $p16^{\text{INK4A}}$  cells<sup>49</sup> (Methods). Consistent with our findings in mice treated with D + Q, reducing the burden of  $p16^{\text{INK4A-hi}}$  cells in 26- to 28-month-old *INK-ATTAC*<sup>+/+</sup> mice also alleviated physical dysfunction (Supplementary Fig. 12b–f).

Testosterone has been reported to alleviate physical dysfunction with aging<sup>50</sup>. To test whether testosterone levels are affected by D + Q, we measured circulating testosterone levels in two cohorts and found no statistically significant differences between the vehicle and D + Q groups (Supplementary Fig. 13). This appears to rule out the potential explanation that improvement of physical function is due to increased testosterone induced by senolytics.

Next, we tested whether eliminating senescent cells using a potentially translatable approach, intermittent treatment with senolytics beginning at very old age, extends remaining lifespan in WT mice (Fig. 6j). Remarkably, mice treated with biweekly administration of D + Q starting at 24–27 months of age (equivalent to a human age of 75–90 years) had a 36% higher median post-treatment lifespan and a lower mortality hazard, 64.9% ( $P=0.01$ ), than the vehicle group (Fig. 6k,l and Supplementary Fig. 14a,b), indicating that senolytics can reduce risk of death in old mice.

To test whether this reduced mortality in old mice comes at the cost of an increased period of late-life morbidity, we assessed physical function in mice treated with D + Q or vehicle monthly until death. Despite the longer remaining lifespan in the D + Q-treated mice, physical function in the last 2 months of life was not lower than that of vehicle-treated mice in males and females (Fig. 6m and

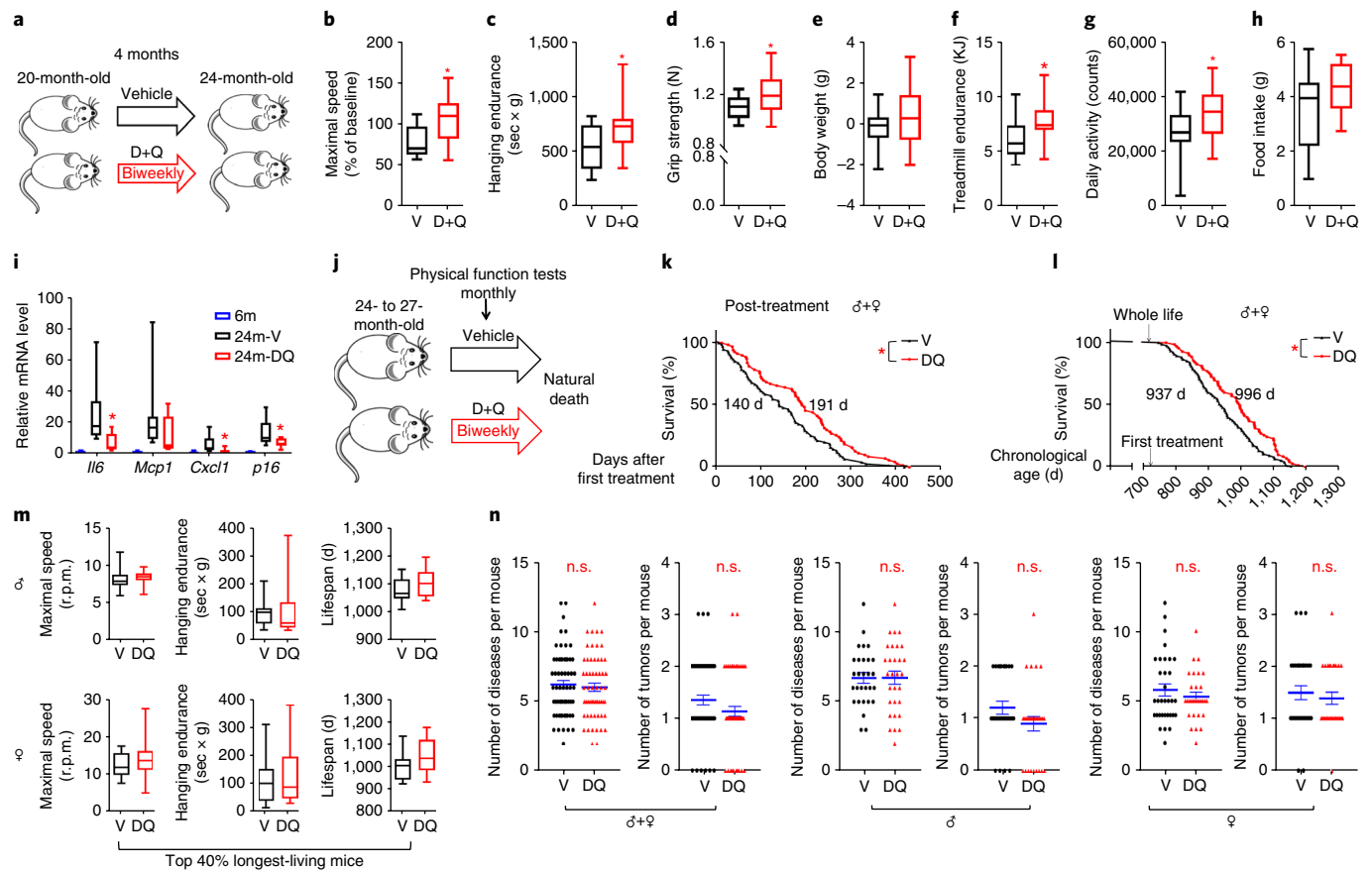


**Fig. 6 | Senolytics extend both health- and lifespan in aged mice.** **a**, Experimental design for physical function measurements in 20-month-old male mice treated with D + Q once every 2 weeks (biweekly) for 4 months. **b–h**, Quantification of maximal walking speed (relative to baseline) (**b**), hanging endurance (**c**), grip strength (**d**), body weight change from baseline (**e**), treadmill endurance (**f**), daily activity (**g**), and food intake (**h**) of 20-month-old male C57BL/6 mice at 4 months after treatment initiation ( $n=20$  for D + Q;  $n=13$  for V). **i**, The relative mRNA abundance for target genes of visceral adipose tissue from 6-month-old nontreated (6 m,  $n=7$ ), 24-month-old vehicle-treated (24m-V,  $n=8$ ), and 24-month-old D + Q-treated (24m-DQ,  $n=8$ ) mice. (**j**) Experimental design for lifespan analyses. **k, l**, Post-treatment survival (**k**) and whole-life survival (**l**) curves of C57BL/6 mice treated biweekly with D + Q ( $n=71$ ; 40 males, 31 females) or vehicle ( $n=76$ ; 41 males, 35 females) starting at 24–27 months of age. Median survival is indicated for all curves. **m**, Maximal walking speed and hanging endurance averaged over the last 2 months of life and lifespan for the longest living mice (top 40%) in both groups for both sexes. For male mice,  $n=12$  for D + Q and  $n=12$  for V. For female mice,  $n=13$  for D + Q and  $n=13$  for V. **n**, Disease burden and tumor burden at death. For both sexes,  $n=59$  for D + Q,  $n=62$  for V. For males,  $n=30$  for D + Q,  $n=29$  for V. For females,  $n=29$  for D + Q,  $n=33$  for V. Results are shown as box-and-whisker plots, where a box extends from the 25th to 75th percentile with the median shown as a line in the middle, and whiskers indicate smallest and largest values (**b–i, m**), or as mean  $\pm$  s.e.m. (**n**). \* $P < 0.05$ ; n.s., not significant; two-tailed Student's *t*-tests (**b–i, m, n**) and Cox proportional hazard regression model (**k, l**).

Supplementary Fig. 14c,d). At autopsy, the prevalence of several age-related diseases, tumor burden, and cause of death were not statistically different between D + Q- and vehicle-treated mice in males and females (Fig. 6n and Supplementary Fig. 15). Thus, orally active senolytic drugs, which reduce the burden of senescent and possibly other cells that have exaggerated inflammatory cytokine production coupled with dependence on prosurvival SCAP pathways, can increase post-treatment lifespan without causing prolonged morbidity in mice, even when administered late in life.

## Discussion

Our study shows that health- and lifespan are curtailed by increased senescent cell abundance and, conversely, are enhanced by reducing proinflammatory, SCAP-dependent senescent cell burden in mice, even late in life. Collectively, evidence for a causal role of such senescent cells in physical dysfunction satisfies a modified set of Koch's postulates<sup>34</sup>: (i) senescent cell burden<sup>14</sup> and physical dysfunction<sup>5</sup> are associated with each other and with aging; (ii) transplanting small numbers of senescent cells into young mice that

have few endogenous senescent cells is sufficient to cause physical dysfunction that lasts for months; (iii) senolytics prevent and alleviate this senescent cell transplantation-induced physical dysfunction in young mice; (iv) clearing senescent cells alleviates physical dysfunction and increases remaining lifespan in old mice; and (v) locally inducing senescence in the lung impaired physical function, and clearing senescent cells improved physical function in a bleomycin-induced pulmonary fibrosis mouse model<sup>25</sup>. Notably, we determined that the total cell number in recipient adipose tissue is approximately 350 million. Several studies have shown that the percentage of senescent cells in adipose tissue from aged animals can be up to 2–10% (refs. 14,15,20), indicating that there might be at least 7 million endogenous senescent cells in adipose tissue of aged mice. Although other mechanisms might contribute, one reason why such a small number (0.5–1 million) of transplanted senescent cells could cause systemic dysfunction is spread of senescence and inflammation locally and to distant tissues.

We used preadipocytes for transplantation, as these cells appear to be less susceptible to immune rejection than other cell types<sup>26</sup>, a



reason for their increasing clinical use in cell transplantation studies. To further test whether there is a role of immune rejection in the physical dysfunction caused by senescent cell transplantation, we performed autologous transplantation, and we also transplanted human senescent cells into immunodeficient (SCID-beige) mice. Senescent cells induced essentially identical physical dysfunction in both of these settings in which immune rejection is greatly reduced. These points, together with our finding that transplanted senescent and control cells disappear at the same rate following transplantation, plus the long-lasting phenotypes caused by transplanting senescent cells, indicate that immune-rejection or transient 'sickness' caused by transplantation might not be a primary cause for the physical dysfunction we found. The SCID-beige mouse senescent cell-transplantation model could pave the way for testing the effects of other senescent cell types that are more immunogenic than preadipocytes or autologous cells in future studies.

We originally discovered that D+Q are senolytic agents by using a hypothesis-driven bioinformatics approach. This approach was based on the hypotheses that senescent cells depend on pro-survival pathways to defend themselves against their proapoptotic microenvironment and that disabling these pathways would therefore selectively kill senescent cells<sup>35</sup>. That D+Q can specifically kill senescent cells in human adipose tissue is supported by the following evidence: (i) D+Q induce apoptosis only in senescent human cells, rather than in control cells *in vitro*<sup>35</sup>; (ii) D+Q significantly decreased senescent cells as determined in three different assessments, whereas D+Q did not reduce the overall number of cells in adipose tissue; and (iii) secretion of two major adipokines was not reduced by D+Q, effectively ruling out nonspecific effects on secretion or cell viability. We believe that these data indicate that occurrence of nonspecific cellular toxicity occurs as a result of D+Q is unlikely. Of note, we showed the effectiveness of senolytics in targeting naturally occurring senescent cells in human adipose tissue explants collected from obese subjects. Although similar to aging, obesity is highly associated with increased senescent cell burden<sup>27,32</sup>. In future studies, the efficacy of senolytics in tissues from older humans needs to be compared to that in explants from obese subjects.

We found that D+Q has little direct effect on macrophages. However, it is unlikely that the substantial reduction of proinflammatory cytokine secretion following D+Q was due to elimination of senescent cells alone. Interestingly, we found that senescent cells can induce adipose tissue cytokine production, potentially amplifying inflammation. By clearing senescent cells, this possible amplification of inflammation could be attenuated in adipose tissue, which includes macrophages. On the basis of these findings, we speculate that by decreasing senescent cell abundance, reduced inflammatory activity in adipose tissue could ensue and contribute to the reduction of inflammation after D+Q exposure, as well as to decreased spread of senescence.

Reducing p16<sup>INK4A-hi</sup> cells, some of which are senescent, in *INK-ATTAC* transgenic mice starting from midadulthood (age 12 months) reportedly extends median lifespan<sup>49</sup>. In our study, administration of D+Q or AP20187 under the same conditions to WT and *INK-ATTAC* mice began at age 24–27 months. Unlike D+Q, AP20187 did not enhance late-life survival. One reason could be that senolytics act by disabling the SCAP, a mechanism of action that is distinct from that in *INK-ATTAC* mice, in which p16<sup>INK4A-hi</sup> cells are targeted. We chose old age (24–27 months) rather than middle age (12 months) to start treatment for several reasons. First, 12-month-old mice are roughly equivalent to 40-year-old humans, and 24-month-old mice are equivalent to 75-year-old humans. We felt that beginning at 24 months of age is potentially a more translatable scenario. Second, AP20187 targets p16<sup>INK4A+</sup> cells, some of which are senescent, but others of which are not<sup>51,52</sup> (e.g., pancreatic  $\beta$ -cells, macrophages, etc.). Considering that 12-month-old

mice have very few detectible senescent cells in adipose tissue, whereas these cells are abundant in 24-month-old mice<sup>20</sup>, beginning AP20187 administration at 12 months of age could have targeted a higher proportion of p16<sup>INK4A+</sup> cells that are not senescent than initiating treatment at 24 months of age, when senescent cells are readily detectible in multiple tissues. Third, treating *INK-ATTAC* mice from 12-month-old mice led to an increase in median rather than maximum survival. This is consistent with our finding that AP20187 did not detectibly increase late-life survival. On the other hand, we show here that by initiating senolytics in later life, late-life survival is actually increased.

Age-related diseases were delayed as a group in old male and female mice treated with D+Q compared to vehicle-treated controls. There was no one disease that was delayed or prevented that alone accounted for this increase in survival. In further support of the hypothesis that senescent cells participate in predisposition to age-related dysfunction, we found that the converse is also the case. Age-related diseases occurred earlier as a group in senescent cell-transplanted mice, coupled with shorter survival, than in control mice not transplanted with senescent cells. No one disease accounted for this decreased survival. These findings are consistent with the geroscience hypothesis: by targeting a fundamental aging process, such as cellular senescence, age-related disorders will be delayed as a group, with no one condition predominating.

Quercetin has been found to alleviate a variety of disorders through diverse mechanisms of action<sup>53</sup>, almost all of which have been studied with uninterrupted dosing, resulting in quercetin being continuously present. This is consistent with the presumption that quercetin acts on specific enzymes or pathways to achieve these effects. However, in our study, we administered D+Q intermittently. Dasatinib and quercetin both have short elimination half-lives<sup>44,45</sup>, supporting the possibility that their beneficial effects on late-life function and survival were at least partially due to a mechanism that persists long after the drugs are no longer present, such as senescent cell elimination. Dasatinib can have side effects, occasionally including serious ones such as pulmonary edema, which can occur after 8–48 months of daily administration<sup>54</sup>. Although recognized side effects of drugs in mice often differ substantially from those in humans, in our study, mice given D+Q intermittently lived longer and had improved physical function compared to vehicle-treated mice. When they eventually died, the pathologies of D+Q-treated mice determined at autopsy and through histological analysis did not differ substantially from those of vehicle-treated mice. Possibly, intermittent treatment with senolytics may serve to reduce potential side effects<sup>55</sup>, an important consideration in the frail elderly, a population vulnerable to adverse drug reactions. We emphasize that preclinical studies to search for potential toxicities and optimized regimens are required before contemplating trials in relatively healthy humans. A search for possible side effects of senolytics as a class and of individual senolytics is especially important.

Our study provides proof-of-concept evidence indicating that targeting senescent cells can improve both health- and lifespan in mice. Because of the role of senescent cells in inducing physical dysfunction in mice demonstrated here (with some similarity to human frailty<sup>4,31,56</sup>), senolytics might prove to be effective in alleviating physical dysfunction and resulting loss of independence in older human subjects, depending on whether these agents turn out to be safe and effective in clinical trials. Depending on the outcomes of such ongoing (ClinicalTrials.gov identifier: NCT02848131) and future preclinical and clinical studies, intermittent administration of senolytics, including newer agents such as optimized derivatives of D+Q, could possibly be useful in enhancing healthspan and remaining survival not only in older subjects, but also in other individuals, such as cancer survivors treated with senescence-inducing radiation or chemotherapy<sup>57</sup>.

## Methods

Methods, including statements of data availability and any associated accession codes and references, are available at <https://doi.org/10.1038/s41591-018-0092-9>.

Received: 11 October 2017; Accepted: 9 May 2018;

Published online: 09 July 2018

## References

- Crimmins, E. M. Lifespan and healthspan: past, present, and promise. *Gerontologist* **55**, 901–911 (2015).
- Fries, J. F. Aging, natural death, and the compression of morbidity. *N. Engl. J. Med.* **303**, 130–135 (1980).
- Michaud, M. et al. Proinflammatory cytokines, aging, and age-related diseases. *J. Am. Med. Dir. Assoc.* **14**, 877–882 (2013).
- Fried, L. P. et al. Frailty in older adults: evidence for a phenotype. *J. Gerontol. A Biol. Sci. Med. Sci.* **56**, M146–M156 (2001).
- Collard, R. M., Boter, H., Schoevers, R. A. & Oude Voshaar, R. C. Prevalence of frailty in community-dwelling older persons: a systematic review. *J. Am. Geriatr. Soc.* **60**, 1487–1492 (2012).
- Song, X., Mitnitski, A. & Rockwood, K. Prevalence and 10-year outcomes of frailty in older adults in relation to deficit accumulation. *J. Am. Geriatr. Soc.* **58**, 681–687 (2010).
- Xue, Q. L. The frailty syndrome: definition and natural history. *Clin. Geriatr. Med.* **27**, 1–15 (2011).
- Tchkonia, T., Zhu, Y., van Deursen, J., Campisi, J. & Kirkland, J. L. Cellular senescence and the senescent secretory phenotype: therapeutic opportunities. *J. Clin. Invest.* **123**, 966–972 (2013).
- Campisi, J. & d'Adda di Fagnana, F. Cellular senescence: when bad things happen to good cells. *Nat. Rev. Mol. Cell Biol.* **8**, 729–740 (2007).
- Wiley, C. D. et al. Mitochondrial dysfunction induces senescence with a distinct secretory phenotype. *Cell Metab.* **23**, 303–314 (2016).
- Wang, C. et al. DNA damage response and cellular senescence in tissues of aging mice. *Aging Cell* **8**, 311–323 (2009).
- Zhu, Y., Armstrong, J. L., Tchkonia, T. & Kirkland, J. L. Cellular senescence and the senescent secretory phenotype in age-related chronic diseases. *Curr. Opin. Clin. Nutr. Metab. Care* **17**, 324–328 (2014).
- Coppé, J. P. et al. Senescence-associated secretory phenotypes reveal cell-nonautonomous functions of oncogenic RAS and the p53 tumor suppressor. *PLoS Biol.* **6**, 2853–2868 (2008).
- Xu, M. et al. JAK inhibition alleviates the cellular senescence-associated secretory phenotype and frailty in old age. *Proc. Natl. Acad. Sci. USA* **112**, E6301–E6310 (2015).
- Xu, M. et al. Targeting senescent cells enhances adipogenesis and metabolic function in old age. *eLife* **4**, e12997 (2015).
- Xu, M. et al. Transplanted senescent cells induce an osteoarthritis-like condition in mice. *J. Gerontol. A Biol. Sci. Med. Sci.* **72**, 780–785 (2017).
- Palmer, A. K. et al. cellular senescence in type 2 diabetes: a therapeutic opportunity. *Diabetes* **64**, 2289–2298 (2015).
- Chang, J. et al. Clearance of senescent cells by ABT263 rejuvenates aged hematopoietic stem cells in mice. *Nat. Med.* **22**, 78–83 (2016).
- Childs, B. G. et al. Senescent intimal foam cells are deleterious at all stages of atherosclerosis. *Science* **354**, 472–477 (2016).
- Baker, D. J. et al. Naturally occurring p16<sup>INK4a</sup>-positive cells shorten healthy lifespan. *Nature* **530**, 184–189 (2016).
- Xu, M., Tchkonia, T. & Kirkland, J. L. Perspective: targeting the JAK/STAT pathway to fight age-related dysfunction. *Pharmacol. Res.* **111**, 152–154 (2016).
- Bitto, A. et al. Transient rapamycin treatment can increase lifespan and healthspan in middle-aged mice. *eLife* **5**, e16351 (2016).
- Tchkonia, T. et al. Mechanisms and metabolic implications of regional differences among fat depots. *Cell Metab.* **17**, 644–656 (2013).
- Farr, J. N. et al. Identification of senescent cells in the bone microenvironment. *J. Bone Miner. Res.* **31**, 1920–1929 (2016).
- Schafer, M. J. et al. Cellular senescence mediates fibrotic pulmonary disease. *Nat. Commun.* **8**, 14532 (2017).
- Ryan, J. M., Barry, F. P., Murphy, J. M. & Mahon, B. P. Mesenchymal stem cells avoid allogeneic rejection. *J. Inflamm. (Lond.)* **2**, 8 (2005).
- Tchkonia, T. et al. Fat tissue, aging, and cellular senescence. *Aging Cell* **9**, 667–684 (2010).
- Acosta, J. C. et al. A complex secretory program orchestrated by the inflammasome controls paracrine senescence. *Nat. Cell Biol.* **15**, 978–990 (2013).
- Nelson, G. et al. A senescent cell bystander effect: senescence-induced senescence. *Aging Cell* **11**, 345–349 (2012).
- Hewitt, G. et al. Telomeres are favoured targets of a persistent DNA damage response in ageing and stress-induced senescence. *Nat. Commun.* **3**, 708 (2012).
- Walston, J. et al. The physical and biological characterization of a frail mouse model. *J. Gerontol. A Biol. Sci. Med. Sci.* **63**, 391–398 (2008).
- Schafer, M. J. et al. Exercise prevents diet-induced cellular senescence in adipose tissue. *Diabetes* **65**, 1606–1615 (2016).
- Mosier, D. E., Stell, K. L., Gulizia, R. J., Torbett, B. E. & Gilmore, G. L. Homozygous scid/scid; beige/beige mice have low levels of spontaneous or neonatal T cell-induced B cell generation. *J. Exp. Med.* **177**, 191–194 (1993).
- Kirkland, J. L. & Tchkonia, T. Cellular senescence: a translational perspective. *EBioMedicine* **21**, 21–28 (2017).
- Zhu, Y. et al. The Achilles' heel of senescent cells: from transcriptome to senolytic drugs. *Aging Cell* **14**, 644–658 (2015).
- Stern, J. H., Rutkowski, J. M. & Scherer, P. E. Adiponectin, leptin, and fatty acids in the maintenance of metabolic homeostasis through adipose tissue crosstalk. *Cell Metab.* **23**, 770–784 (2016).
- Farmer, S. R. Transcriptional control of adipocyte formation. *Cell Metab.* **4**, 263–273 (2006).
- Reuben, D. B., Judd-Hamilton, L., Harris, T. B. & Seeman, T. E. The associations between physical activity and inflammatory markers in high-functioning older persons: MacArthur Studies of Successful Aging. *J. Am. Geriatr. Soc.* **51**, 1125–1130 (2003).
- Cohen, H. J., Pieper, C. F., Harris, T., Rao, K. M. & Currie, M. S. The association of plasma IL-6 levels with functional disability in community-dwelling elderly. *J. Gerontol. A Biol. Sci. Med. Sci.* **52**, M201–M208 (1997).
- Beyer, I. et al. Inflammation-related muscle weakness and fatigue in geriatric patients. *Exp. Gerontol.* **47**, 52–59 (2012).
- Lu, Y. et al. Inflammatory and immune markers associated with physical frailty syndrome: findings from Singapore longitudinal aging studies. *Oncotarget* **7**, 28783–28795 (2016).
- Kao, T. W. et al. Examining how p16<sup>INK4a</sup> expression levels are linked to handgrip strength in the elderly. *Sci. Rep.* **6**, 31905 (2016).
- Justice, J. N. et al. Cellular senescence biomarker p16<sup>INK4a</sup> cell burden in thigh adipose is associated with poor physical function in older women. *J. Gerontol. A Biol. Sci. Med. Sci.* **73**, 939–945 (2017).
- Christopher, L. J. et al. Metabolism and disposition of dasatinib after oral administration to humans. *Drug Metab. Dispos.* **36**, 1357–1364 (2008).
- Graefe, E. U. et al. Pharmacokinetics and bioavailability of quercetin glycosides in humans. *J. Clin. Pharmacol.* **41**, 492–499 (2001).
- Roos, C. M. et al. Chronic senolytic treatment alleviates established vasomotor dysfunction in aged or atherosclerotic mice. *Aging Cell* **15**, 973–977 (2016).
- Farr, J. N. et al. Targeting cellular senescence prevents age-related bone loss in mice. *Nat. Med.* **23**, 1072–1079 (2017).
- Ogrodnik, M. et al. Cellular senescence drives age-dependent hepatic steatosis. *Nat. Commun.* **8**, 15691 (2017).
- Baker, D. J. et al. Clearance of p16<sup>INK4a</sup>-positive senescent cells delays ageing-associated disorders. *Nature* **479**, 232–236 (2011).
- Srinivas-Shankar, U. & Wu, F. C. Frailty and muscle function: role for testosterone? *Front. Horm. Res.* **37**, 133–149 (2009).
- Hall, B. M. et al. p16<sup>INK4a</sup> and senescence-associated  $\beta$ -galactosidase can be induced in macrophages as part of a reversible response to physiological stimuli. *Aging (Albany NY)* **9**, 1867 (2017).
- Helman, A. et al. p16<sup>INK4a</sup>-induced senescence of pancreatic beta cells enhances insulin secretion. *Nat. Med.* **22**, 412–420 (2016).
- Costa, L. G., Garrick, J. M., Roqué, P. J. & Pellacani, C. Mechanisms of neuroprotection by quercetin: counteracting oxidative stress and more. *Oxid. Med. Cell. Longev.* **2016**, 2986796 (2016).
- Montani, D. et al. Pulmonary arterial hypertension in patients treated by dasatinib. *Circulation* **125**, 2128–2137 (2012).
- Kirkland, J. L., Tchkonia, T., Zhu, Y., Niedernhofer, L. J. & Robbins, P. D. The clinical potential of senolytic drugs. *J. Am. Geriatr. Soc.* **65**, 2297–2301 (2017).
- Kane, A. E. et al. Animal models of frailty: current applications in clinical research. *Clin. Interv. Aging* **11**, 1519–1529 (2016).
- Ness, K. K. et al. Frailty in childhood cancer survivors. *Cancer* **121**, 1540–1547 (2015).

## Acknowledgements

The authors are grateful to J. L. Armstrong and L. Thesing for administrative assistance, M. Mahlman for obtaining human adipose tissue samples, Z. Aversa for help with muscle analysis, the Pathology Research Core Lab at Mayo Clinic–Rochester for histology studies, and C. Guo for overall support. This work was supported by the Connor Group (J.L.K.) and Robert J. and Theresa W. Ryan (J.L.K.); the National Institutes of Health (NIH) grants AG13925 (J.L.K.), AG49182 (J.L.K.), DK50456 (Adipocyte Subcore, J.L.K.), AG46061 (A.K.P.), AG004875 (S.K.), AG048792 (S.K.), AR070241 (J.N.F.), AR070281 (M.M.W.), AG13319 (Y.I. and G.B.H.), AG050886 (D.B.A.), AG043376 (P.D.R., and L.J.N.), AG056278 (P.D.R. and L.J.N.), and AG044376 (L.J.N.); a Glenn/American Federation for Aging Research (AFAR) BIG Award (J.L.K.); the Glenn Foundation (L.J.N.); and the Ted Nash Long Life and Noaber Foundations (J.L.K.). M.X. received the

Glenn/AFAR Postdoctoral Fellowship for Translational Research on Aging and an Irene Diamond Fund/AFAR Postdoctoral Transition Award in Aging.

### Author contributions

M.X., T.T., and J.L.K. conceived and designed the study. M.X. performed and analyzed most of the transplanted mouse experiments and human adipose tissue explant experiments. N.G. and T.T. contributed to the human adipose tissue explant experiments. J.N.F., D.G.E., J.L.O., and S.K. contributed to the study of aged mice treated with senolytics. A.K.P. contributed to the bioluminescence studies. M.B.O. and D.J. contributed to ear fibroblast isolation. T.P., M.X., T.T., and C.L.I. performed the survival experiments using senolytics in aged mice. B.M.W., M.M.W., C.M.H., N.K.L., H.C., V.D.G., X.H., S.J.W., K.O.J., M.W., L.G.P.L., G.C.V., P.D.R., L.J.N., and J.D.M. contributed to the mouse studies. R.J.S. contributed to androgen measurement. D.B.A. and K.E. contributed to lifespan analysis. G.B.H. and Y.I. contributed to mouse pathology analysis. M.X. and J.L.K. wrote the manuscript with input from all coauthors. J.L.K., M.X., and T.T. oversaw all experimental design, data analyses, and manuscript preparation.

### Competing interests

J.L.K., T.T., M.X., T.P., N.G., and A.K.P. have a financial interest related to this research. Patents on senolytic drugs (PCT/US2016/041646, filed at the US Patent Office) are held by Mayo Clinic. This research has been reviewed by the Mayo Clinic Conflict of Interest Review Board and was conducted in compliance with Mayo Clinic Conflict of Interest policies. None of the other authors has a relevant financial conflict of interest.

### Additional information

**Supplementary information** is available for this paper at <https://doi.org/10.1038/s41591-018-0092-9>.

**Reprints and permissions information** is available at [www.nature.com/reprints](http://www.nature.com/reprints).

**Correspondence and requests for materials** should be addressed to M.X. or T.T. or J.L.K.

**Publisher's note:** Springer Nature remains neutral with regard to jurisdictional claims in published maps and institutional affiliations.

## Methods

**Mouse models and drug treatments.** All animal experiments were performed according to protocols approved by the Institutional Animal Care and Use Committee (IACUC) at Mayo Clinic. Wild-type C57BL/6 mice were obtained from the National Institute on Aging (NIA) and maintained in a pathogen-free facility at 23–24 °C under a 12-h light, 12-h dark regimen with free access to a NCD (standard mouse diet with 20% protein, 5% fat (13.2% fat by calories), and 6% fiber; Lab Diet 5053, St. Louis, MO) and water. Quarterly testing was negative for the following pathogens: *Clostridium piliforme*, *Mycoplasma pulmonis*, cilia-associated respiratory (CAR) bacillus, ectromelia, rotavirus (EDIM), Hantaan virus, K virus, lymphocytic choriomeningitis virus (LCMV), lactate dehydrogenase-elevating virus (LDEV), mouse adenovirus 1 and 2, mouse cytomegalovirus (MCMV), mouse hepatitis virus (MHV), minute virus of mice (MVM), mouse parvovirus (MPV), mouse thymic virus (MTV), polyomavirus, pneumonia virus of mice (PVM), REO-3 virus, Sendai virus, *Mycoplasma*, Theiler's murine encephalomyelitis virus (TMEV), *Encephalitozoon cuniculi*, *Aspiculuris tetraptera*, *Radfordia/myobia*, and *Syphacia obvelata*. All mice were fed normal chow unless otherwise indicated. For high-fat feeding, a 60% (by calories) fat diet (D12492, irradiated; Research Diets, New Brunswick, NJ) was used. All mice were housed in static autoclaved HEPA-ventilated microisolation cages (27 × 16.5 × 15.5 cm) with autoclaved Enrich-o-Cobs (The Andersons Incorporated) for bedding. Cages and bedding were changed biweekly. Cages were opened only in class II biosafety cabinets.

Luciferase transgenic C57BL/6 mice were obtained from The Jackson Laboratory (Bar Harbor, ME; stock no. 025854) that express firefly luciferase driven by the constitutively active CAG promoter in most tissues. SCID beige mice (C.B.-17/lcrHsd-Prkd<sup>csid</sup>Lys<sup>flbe-1</sup>) were purchased from ENVIGO (Huntingdon, Cambridgeshire, United Kingdom). T.T., J.L.K., J. van Deursen (Mayo), and D. Baker (Mayo) devised the strategy for and developed *INK-ATTAC* mice<sup>49</sup>. In *INK-ATTAC* mice, the expression of ATTAC, a previously reported construct<sup>38</sup>, is driven by a senescence-activated *p16<sup>INK4A</sup>* promoter sequence. AP20187, a drug that does not appear to affect cells lacking the ATTAC fusion protein, cross-links the mutated FKBP components of ATTAC, allowing the caspase-8 components to be activated through dimerization, leading to apoptosis of cells with high *p16<sup>INK4A</sup>* expression, which includes many senescent cells. These *INK-ATTAC* mice were then bred onto a C57BL/6 background (in the Van Deursen laboratory), genotyped (in the Kirkland laboratory), and aged to 24–27 months (in the Kirkland laboratory). For the lifespan study, AP20187 (B/B homodimerizer, 10 mg per kg body weight (mg/kg)) was injected intraperitoneally into *INK-ATTAC*<sup>+/-</sup> or WT mice daily for 3 consecutive days during each treatment course. We repeated these 3-d treatment courses every 2 weeks. *INK-ATTAC*<sup>+/-</sup> and WT mice (24–27 months old) were age-matched littermates. AP20187 was purchased from Clontech (Mountain View, CA). For all D + Q treatments, dasatinib (5 mg/kg) and quercetin (50 mg/kg) were administered via oral gavage in 100–150 μL 10% PEG400. For treating 20-month-old mice, D + Q treatment was delivered either once monthly or every 2 weeks, with essentially identical effects. For the lifespan study, 24- to 27-month-old mice were treated with D + Q or vehicle for 3 consecutive days every 2 weeks. Dasatinib was purchased from LC Laboratories (Woburn, MA). Quercetin and doxorubicin were purchased from Sigma-Aldrich (St. Louis, MO). All other reagents were purchased from Thermo Fisher Scientific (Waltham, MA) unless indicated otherwise.

**Lifespan studies.** For cell transplantation studies, 16-month-old male C57BL/6 mice were obtained from the National Institute on Aging (NIA). There were 4 or 5 mice housed per cage. We first sorted mice by body weight from low to high. We then selected pairs of mice with similar body weights. Next, either senescent- or control-transplant treatments were assigned to every other mouse using a random number generator, with the intervening mice being assigned to the other treatment, so that pairs of senescent- and control-transplanted mice were matched by weight. After 1 month of acclimation to the animal facility at Mayo Clinic, mice aged 17 months were transplanted with cells. Physical function tests were performed 1 month after transplantation, when mice were aged 18 months. After that, no further tests were performed on these mice except for checking their cages. The earliest death occurred approximately 2 months after the last physical function test. For D + Q studies, 19- to 21-month-old C57BL/6 mice were obtained from the NIA. There were 3–5 mice housed per cage. As with the transplanted mice, mice were sorted on the basis of body weight and randomly assigned to D + Q or vehicle treatment by a person unaware of the study design. Starting at age 24–27 months, mice were treated every 2 weeks with D + Q or vehicle by oral gavage for 3 consecutive days. Some of the mice were moved from their original cages during the course of the study to minimize single cage-housing stress. RotaRod and hanging tests were conducted monthly because these tests are sensitive and noninvasive. We euthanized mice and scored them as having died if they exhibited more than one of the following signs<sup>59</sup>: (i) unable to drink or eat; (ii) reluctant to move even with stimulus; (iii) rapid weight loss; (iv) severe balance disorder; or (v) bleeding or ulcerated tumor. No mouse was lost because of fighting, accidental death, or dermatitis. The Cox proportional hazard model was used for survival analyses.

**Postmortem pathological examination.** Cages were checked every day, and dead mice were removed from cages. Within 24 h, the dead bodies were opened (abdominal cavity, thoracic cavity, and skull) and preserved in 10% formalin individually for at least 7 d. Decomposed or disrupted bodies were excluded. The preserved bodies were shipped to Y.I. for pathological examination. The pathological assessment has been described previously<sup>60</sup>. Briefly, tumor burden (the sum of different types of tumors in each mouse), disease burden (the sum of different histopathological changes of major organs in each mouse), severity of each lesion, and inflammation (lymphocytic infiltrate) were assessed.

**Cell culture.** Mouse preadipocytes (also termed adipose-derived stem cells or adipocyte progenitors) were isolated as described previously<sup>61</sup>. Briefly, after euthanasia, inguinal fat depots were removed under sterile conditions from mice. Adipose tissue was cut into small pieces, digested in collagenase (1 mg/ml) for 60 min at 37 °C, and then filtered through a 100-μm nylon mesh. After centrifugation at 1,000 r.p.m. for 10 min, cell pellets were washed with PBS once and plated in α-MEM containing 10% FBS and antibiotics. After 12 h, adherent preadipocytes were washed, trypsinized, and replated in order to reduce potential endothelial cell and macrophage contamination. Ear fibroblasts were isolated as described previously<sup>62</sup>.

**Whole-mouse DNA determination.** All major organs, except intestine (to exclude microbiota), and the whole skeleton from 5-month-old mice were lysed in lysis buffer (100 mM Tris-HCl, pH 8.8; 5 mM EDTA, pH 8.0; 0.2% SDS; 200 mM NaCl; 100 μg/ml proteinase K) via rotation (10 r.p.m.) at 60 °C for 1 week. Most tissues, except for some bone, were digested. Total DNA per mouse was  $45.5 \pm 3.6$  mg (mean  $\pm$  s.d.;  $n = 3$ ). The molecular weight of the whole mouse genome is  $1.8 \times 10^{12}$  Da, which is equivalent to:  $(1.8 \times 10^{12}) \times (1.67 \times 10^{-24}) = 3 \times 10^{-12}$  g. Therefore, each diploid mouse cell has at least  $6 \times 10^{-12}$  g DNA, and a 5-month-old mouse has at least  $7 \times 10^9$ – $8 \times 10^9$  diploid cells. Using the same method, we estimate that intraperitoneal adipose tissue from a mouse contains  $\sim 3.5 \times 10^8$ – $6 \times 10^8$  diploid cells. Using average body weight, we estimate that there is total of  $\sim 7.5 \times 10^9$ – $8.7 \times 10^9$  diploid cells throughout the body of a 17-month-old mouse.

**Cell transplantation.** To induce senescence in cells to be transplanted, we used radiation or doxorubicin as opposed to serial passaging because: (i) the radiation and chemotherapy frequently used for treating cancers can be associated with frailty<sup>27</sup>; (ii) serially passaging mouse primary cells can induce spontaneous immortalization of mouse cells, effectively ruling out their use for transplantation<sup>63</sup>; and (iii) the SASP of radiation-induced senescent preadipocytes resembles that of serially passaged senescent preadipocytes<sup>14</sup>. Senescence was induced by 10 Gy of cesium radiation or 0.2 mM doxorubicin for 24 h as described previously<sup>14,15</sup>. We mainly used radiation-induced senescent cells in our studies unless indicated otherwise. We considered these cells to be senescent at 20 d after these treatments<sup>14</sup>. More than 85% of cells were senescent as determined on the basis of two assays. Senescent or control cells were collected by trypsinization. Cell pellets were washed with PBS once and resuspended in PBS for transplantation. Mice were anesthetized using isoflurane and cells were injected intraperitoneally in 150 μL PBS through a 22-G needle. We observed that injection using 22-G needles did not interfere with the viability of senescent or control cells.

**Bioluminescence imaging.** Mice were injected intraperitoneally with 3 mg D-luciferin (Gold Biotechnology, St. Louis, MO) in 200 μL PBS. Mice were anesthetized using isoflurane, and bioluminescence images were acquired using a Xenogen Ivis 200 System (Caliper Life Sciences, Hopkinton, MA) according to the manufacturer's instructions.

**Physical function measurements.** All measurements were performed at least 5 d after the last dose of D + Q treatment. Maximal walking speed was assessed using an accelerating RotaRod system (TSE system, Chesterfield, MO). Mice were trained on the RotaRod for 3 d at speeds of 4, 6, and 8 r.p.m. for 200 s on days 1, 2, and 3. On the test day, mice were placed onto the RotaRod, which was started at 4 r.p.m. The rotating speed was accelerated from 4 to 40 r.p.m. over a 5-min interval. The speed was recorded when the mouse dropped off the RotaRod. Results were averaged from 3 or 4 trials and normalized to the baseline speed. Training was not repeated for mice that had been trained within the preceding 2 months. Forelimb grip strength (N) was determined using a Grip Strength Meter (Columbus Instruments, Columbus, OH). Results were averaged over ten trials. For the hanging test, mice were placed onto a 2-mm-thick metal wire that was 35 cm above a padded surface. Mice were allowed to grab the wire with their forelimbs only. Hanging time was normalized to body weight as hanging duration (sec) × body weight (g). Results were averaged from 2 or 3 trials for each mouse. A Comprehensive Laboratory Animal Monitoring System (CLAMS) was used to monitor daily activity and food intake over a 24-h period (12-h light and 12-h dark). The CLAMS system was equipped with an Oxyman Open Circuit Calorimeter System (Columbus Instruments). For treadmill performance, mice were acclimated to a motorized treadmill at an incline of 5° (Columbus Instruments) over 3 d for 5 min each day, starting at a speed of 5 m/min for 2 min and progressing to 7 m/min for 2 min and then 9 m/min for 1 min. On the test

day, mice ran on the treadmill at an initial speed of 5 m/min for 2 min, and then the speed was increased by 2 m/min every 2 min until the mice were exhausted. Exhaustion was defined as the inability to return onto the treadmill despite a mild electrical shock stimulus and mechanical prodding. Distance was recorded and total work (kJ) was calculated using the following formula:  $\text{mass (kg)} \times g (9.8 \text{ m/s}^2) \times \text{distance (m)} \times \sin(5^\circ)$ .

**Real-time PCR.** TRIzol was used to extract RNA from tissues. RNA was reverse-transcribed to cDNA using a M-MLV Reverse Transcriptase kit (Thermo Fisher Scientific) following the manufacturer's instructions. TaqMan fast advanced master mix (Thermo Fisher Scientific) was used for real-time PCR. TATA-binding protein (TBP) was used as an internal control. Probes and primers (TBP, Mm01277042\_m1; IL-6, Mm00446191\_m1; TNF- $\alpha$ , Mm00443260\_g1; *p16<sup>INK4a</sup>*, Mm00944449\_m1; *p21<sup>Cip1</sup>*, Mm04205640\_g1) were purchased from Thermo Fisher Scientific.

**Testosterone assay.** Circulating testosterone was assayed by liquid chromatography–tandem mass spectrometry (LC–MS/MS) (Agilent Technologies, Santa Clara, CA 95051). Intra-assay coefficients of variation (c.v.) were 7.4%, 6.1%, 9.0%, 2.3%, and 0.9% at 0.65, 4.3, 48, 118, and 832 ng/dl, respectively. Interassay c.v. values were 8.9%, 6.9%, 4.0%, 3.6%, and 3.5% at 0.69, 4.3, 45, 117, and 841 ng/dl, respectively.

**Human adipose tissue explants.** The protocol was approved by the Mayo Clinic Foundation Institutional Review Board for Human Research. Informed consent was obtained from all subjects. Human adipose tissue was resected during gastric bypass surgery from eight obese subjects. Two of the subjects were male, and six were female. The mean age of the subjects was  $45.8 \pm 8.2$  years (mean  $\pm$  s.d.; range, 36–58). Mean BMI was  $45.5 \pm 9.1$  kg/m<sup>2</sup> (mean  $\pm$  s.d.; range, 38–66). No subject was known to have a malignancy. Greater omental adipose tissue was obtained from each subject. Adipose tissue was cut into small pieces and washed with PBS three times. Adipose tissue was then cultured in medium containing 1 mM sodium pyruvate, 2 mM glutamine, MEM vitamins, MEM nonessential amino acids, and antibiotics with 20  $\mu$ M quercetin and 1  $\mu$ M dasatinib or DMSO. After 48 h, the adipose explants were washed three times with PBS. Aliquots of adipose tissue were fixed for immunostaining or SA- $\beta$ gal assay. The rest of the tissue was maintained in the same medium without drugs for 24 h to collect CM for multiplex protein analysis. For Supplementary Fig. 10, CM was collected from human senescent primary preadipocytes, control preadipocytes, and blank culture flasks containing no cells (Blank CM). senescent and control preadipocytes were obtained from the same donor. Human subcutaneous adipose tissue explants were obtained from a lean kidney donor (BMI, 26.5 kg/m<sup>2</sup>; age, 43 years) and divided into pieces. These explants were incubated with senescent, control, or Blank CM for 24 h. Next, these explants were washed with PBS and then incubated with fresh medium for conditioning for another 24 h.

**Multiplex protein analyses.** Proinflammatory cytokine and chemokine protein levels in CM were measured using Luminex xMAP technology. The multiplexing analysis was performed using the Luminex 100 system (Luminex, Austin, TX) by Eve Technologies Corp. (Calgary, Alberta, Canada). Human multiplex kits were from Millipore (Billerica, MA).

**SA- $\beta$ gal assay and immunostaining.** Adipose tissue cellular SA- $\beta$ gal activity was assayed as previously described<sup>14</sup>. TAF immunofluorescence in situ hybridization was performed as described previously<sup>30</sup>. Briefly, formalin-fixed, paraffin-embedded (FFPE) adipose tissue blocks were cut into 5- $\mu$ m sections. Sections were deparaffinized with HistoClear (National Diagnostics, Charlotte, NC) and hydrated using an ethanol gradient. Antigen was retrieved by incubation in 0.01 M, pH 6.0 citrate serum or horse serum 1:60 in 0.1% BSA in PBS) for 60 min at room temperature. Samples were further blocked with avidin–biotin (Vector Lab, Burlingame, CA) for 15 min at room temperature. Primary antibody (anti- $\gamma$ H2AX 1:200, Cell Signaling, Danvers, MA, catalog no. 9718) was applied overnight at 4 °C in the blocking buffer. Washed slides were then incubated for 30 min with biotinylated, anti-rabbit secondary antibody (Vector Lab, catalog no. BA-1000). Finally, fluorescein-labeled avidin DCS (Vector Lab) was applied for 20 min. For luciferase costaining, a second primary antibody (anti-luciferase 1:500, Novusbio, Littleton, CO, catalog no. NB100-1677SS) was applied overnight at 4 °C in blocking buffer. Next, washed slides were incubated with secondary antibody (Alexa Fluor 647 1:500, Thermo Fisher Scientific, catalog no. A-21447). Telomeres were then stained by fluorescent in situ hybridization (FISH). Slides were fixed with 4% paraformaldehyde for 20 min, dehydrated in an alcohol gradient cascade, and denatured for 10 min at 80 °C in hybridization buffer (70% formamide (Sigma-Aldrich), 25 mM MgCl<sub>2</sub>,

1 M Tris pH 7.2, 5% blocking reagent (Roche, Basel, Switzerland)) with a 2.5  $\mu$ g/ml Cy-3-labeled telomere-specific (CCCTAA) peptide nucleic acid probe (Panagene, Daejeon, Korea) for 2 h at room temperature in the dark. After washing, sections were incubated with DAPI, mounted, and imaged. In-depth Z-stacking (a minimum of 20 optical slices with 100 $\times$  oil objective) was used for imaging. The images were further processed using Huygens (SVI) deconvolution. Immunohistochemical (IHC) staining was performed by the Pathology Research Core (Mayo Clinic, Rochester, MN) using a Leica Bond RX stainer (Leica, Buffalo Grove, IL). Slides were retrieved for 20 min using Epitope Retrieval 1 (Citrate; Leica) and incubated in Protein Block (Dako, Agilent, Santa Clara, CA) for 5 min. Primary antibodies were diluted in Background Reducing Diluent (Dako) as follows: p16<sup>INK4A</sup> (rabbit, monoclonal; Abcam, Cambridge, MA, catalog no. ab108349) at 1:600, cleaved-caspase 3 (rabbit, polyclonal; Cell Signaling, catalog no. 9661L) at 1:200, and F4/80 (rat, monoclonal; Abcam, catalog no. ab90247) at 1:500, except for CD68 antibody (mouse, monoclonal; Dako, catalog no. M0876), which was diluted in Bond Diluent (Leica) at 1:200. All primary antibodies were diluted in Background Reducing Diluent (Dako) and incubated for 15 min. The detection system used was a Polymer Refine Detection System (Leica). This system includes the hydrogen peroxidase block, post primary and polymer reagent, DAB, and hematoxylin. Immunostaining visualization was achieved by incubating the slides for 10 min in DAB and DAB buffer (1:19 mixture) from the Bond Polymer Refine Detection System. Slides were counterstained for 5 min using Schmidt hematoxylin, followed by several rinses in 1 $\times$  Bond wash buffer and distilled water. Slides were dehydrated using increasing concentrations of ethyl alcohol and cleared by three changes of xylene before permanent coverslipping in xylene-based medium.

**Statistical analysis.** GraphPad Prism 7.0 was used for most statistical analyses. Two-tailed Student's *t*-tests were used to estimate statistically significant differences between two groups. One-way ANOVA with Tukey's *post hoc* comparison was used for multiple comparisons. Pearson's correlation coefficients were used to test correlations. As mice were obtained in several cohorts and grouped in cages, the Cox proportional hazard model was used for survival analyses. The model incorporated sex and age of treatment as fixed effects and cohorts and initial cage assignment as random effects. Because of the fact that some of mice were moved from their initial cages during the study to minimize stress from single-cage housing, we also conducted analyses without cage effect. Results between these two analyses did not differ substantially in directionality or statistical significance, strengthening confidence in our results. Survival analysis was performed using statistical software R (version 3.4.1; library 'coxme'). Investigators were blinded to allocation during most of experiments and outcome assessments. We used baseline body weight to assign mice to experimental groups (to achieve similar body weight between groups), so only randomization within groups matched by body weight was conducted. We determined the sample size based on our previous experiments, so no statistical power analysis was used. Values are presented as mean  $\pm$  s.e.m. unless otherwise indicated, with *P* < 0.05 considered to be significant. All replicates in this study were from different samples, each isolated from different mice or human subjects.

**Reporting Summary.** Further information on experimental design is available in the Nature Research Reporting Summary linked to this article.

**Data Availability.** Source data are available for Figs. 1–6. Reasonable requests for other data presented in this manuscript will be honored by the corresponding authors.

## References

- Pajvani, U. B. et al. Fat apoptosis through targeted activation of caspase 8: a new mouse model of inducible and reversible lipodystrophy. *Nat. Med.* **11**, 797–803 (2005).
- Miller, R. A. et al. An aging interventions testing program: study design and interim report. *Aging Cell* **6**, 565–575 (2007).
- Ikeno, Y. et al. Housing density does not influence the longevity effect of calorie restriction. *J. Gerontol. A Biol. Sci. Med. Sci.* **60**, 1510–1517 (2005).
- Tchkonia, T. et al. Increased TNF $\alpha$  and CCAAT/enhancer-binding protein homologous protein with aging predispose preadipocytes to resist adipogenesis. *Am. J. Physiol. Endocrinol. Metab.* **293**, E1810–E1819 (2007).
- Jurk, D. et al. Chronic inflammation induces telomere dysfunction and accelerates ageing in mice. *Nat. Commun.* **2**, 4172 (2014).
- Xu, J. Preparation, culture, and immortalization of mouse embryonic fibroblasts. *Curr. Protoc. Mol. Biol.* **70**, 28.1.1–28.1.8 (2005).

## Life Sciences Reporting Summary

Nature Research wishes to improve the reproducibility of the work that we publish. This form is intended for publication with all accepted life science papers and provides structure for consistency and transparency in reporting. Every life science submission will use this form; some list items might not apply to an individual manuscript, but all fields must be completed for clarity.

For further information on the points included in this form, see [Reporting Life Sciences Research](#). For further information on Nature Research policies, including our [data availability policy](#), see [Authors & Referees](#) and the [Editorial Policy Checklist](#).

### ▶ Experimental design

#### 1. Sample size

Describe how sample size was determined.

Sample sizes were determined based on the means and variation of previous pilot or published experiments.

#### 2. Data exclusions

Describe any data exclusions.

No data were excluded.

#### 3. Replication

Describe whether the experimental findings were reliably reproduced.

All the key findings were reliably reproduced in several independent cohorts with large N's.

#### 4. Randomization

Describe how samples/organisms/participants were allocated into experimental groups.

We used baseline body weight to assign animals to experimental groups (to achieve similar body weight between groups), so only randomization (using a random number generator in Excel) within groups matched by body weight was conducted.

#### 5. Blinding

Describe whether the investigators were blinded to group allocation during data collection and/or analysis.

Investigators were blinded to allocation during experiments and outcome assessments.

Note: all studies involving animals and/or human research participants must disclose whether blinding and randomization were used.

#### 6. Statistical parameters

For all figures and tables that use statistical methods, confirm that the following items are present in relevant figure legends (or in the Methods section if additional space is needed).

- |                          |  |
|--------------------------|--|
| n/a                      | Confirmed  |
| <input type="checkbox"/> | <input checked="" type="checkbox"/> The <u>exact sample size</u> ( $n$ ) for each experimental group/condition, given as a discrete number and unit of measurement (animals, litters, cultures, etc.)                                    |
| <input type="checkbox"/> | <input checked="" type="checkbox"/> A description of how samples were collected, noting whether measurements were taken from distinct samples or whether the same sample was measured repeatedly   |
| <input type="checkbox"/> | <input checked="" type="checkbox"/> A statement indicating how many times each experiment was replicated   |
| <input type="checkbox"/> | <input checked="" type="checkbox"/> The statistical test(s) used and whether they are one- or two-sided (note: only common tests should be described solely by name; more complex techniques should be described in the Methods section) |
| <input type="checkbox"/> | <input checked="" type="checkbox"/> A description of any assumptions or corrections, such as an adjustment for multiple comparisons  |
| <input type="checkbox"/> | <input checked="" type="checkbox"/> The test results (e.g. $P$ values) given as exact values whenever possible and with confidence intervals noted   |
| <input type="checkbox"/> | <input checked="" type="checkbox"/> A clear description of statistics including <u>central tendency</u> (e.g. median, mean) and <u>variation</u> (e.g. standard deviation, interquartile range)  |
| <input type="checkbox"/> | <input checked="" type="checkbox"/> Clearly defined error bars   |

See the web collection on [statistics for biologists](#) for further resources and guidance.

## ► Software

Policy information about [availability of computer code](#)

### 7. Software

Describe the software used to analyze the data in this study.

Data were analyzed using Prism 7 for Mac OS X (Graphpad, Inc.).

For manuscripts utilizing custom algorithms or software that are central to the paper but not yet described in the published literature, software must be made available to editors and reviewers upon request. We strongly encourage code deposition in a community repository (e.g. GitHub). *Nature Methods* [guidance for providing algorithms and software for publication](#) provides further information on this topic.

## ► Materials and reagents

Policy information about [availability of materials](#)

### 8. Materials availability

Indicate whether there are restrictions on availability of unique materials or if these materials are only available for distribution by a for-profit company.

To obtain INK-ATTAC mice, interested parties should contact J.L. Kirkland at Mayo Clinic.

### 9. Antibodies

Describe the antibodies used and how they were validated for use in the system under study (i.e. assay and species).

All antibodies were commercially available and validated by the companies. For immunohistochemistry, the antibodies were further validated by the Pathology Research Core at Mayo Clinic using positive and negative controls from human or mouse tissues.  $\gamma$ H2AX, F4/80, and luciferase antibodies were further validated with proper positive and negative controls. All antibody information was included in the Online Methods.

### 10. Eukaryotic cell lines

a. State the source of each eukaryotic cell line used.

No cell line was used.

b. Describe the method of cell line authentication used.

No cell line was used.

c. Report whether the cell lines were tested for mycoplasma contamination.

All primary cells were tested weekly for mycoplasma and were negative.

d. If any of the cell lines used are listed in the database of commonly misidentified cell lines maintained by [ICLAC](#), provide a scientific rationale for their use.

N/A

## ► Animals and human research participants

Policy information about [studies involving animals](#); when reporting animal research, follow the [ARRIVE guidelines](#)

### 11. Description of research animals

Provide details on animals and/or animal-derived materials used in the study.

Both male and female C57BL/6 mice were used for transplantation and D+Q treatment. The ages of mice were clearly indicated in both Results and Figure Legends. We also isolated primary preadipocytes and ear fibroblasts from 5-8 month old C57BL/6 male or female mice. Detailed information about these mice was included in figure legends. Luciferase transgenic C57BL/6 mice were obtained from the Jackson Laboratory (Bar Harbor, ME; Stock No: 025854). INK-ATTAC transgenic mice were previously generated and bred onto a C57BL/6 background as described in the Online Methods.

Policy information about [studies involving human research participants](#)

### 12. Description of human research participants

Describe the covariate-relevant population characteristics of the human research participants.

Human adipose tissue was resected during gastric bypass surgery from 8 obese subjects. Two of the subjects were male and 6 were female. Ages of subjects were  $45.8 \pm 8.2$  years (means  $\pm$  SD; range 36–58). Mean body mass index (BMI) was  $45.5 \pm 9.1$  kg/m<sup>2</sup> (means  $\pm$  SD; range 38–66). No subject was known to have a malignancy. Greater omental adipose tissue was obtained from each subject.